TURUN
YLIOPISTO
UNIVERSITY
OF TURKU

Multifunctional light-responsive textiles

and their sustainable development

Alicja Ławrynowicz

TURUN YLIOPISTON JULKAISUJA – ANNALES UNIVERSITATIS TURKUENSIS
SARJA – SER. F OSA – TOM. 69 | TECHNICA – INFORMATICA | TURKU 2025

TURUN
YLIOPISTO
UNIVERSITY
OF TURKU

MULTIFUNCTIONAL LIGHT-RESPONSIVE TEXTILES

and their sustainable development

Alicja Ławrynowicz

TURUN YLIOPISTON JULKAISUJA – ANNALES UNIVERSITATIS TURKUENSIS
SARJA – SER. F OSA – TOM. 69 | TECHNICA – INFORMATICA | TURKU 2025

University of Turku

Faculty of Technology
Department of Mechanical and Materials Engineering
Materials Engineering
Doctoral Programme in Technology (DPT)

Supervised by

Professor Kati Miettunen
University of Turku
Turku, Finland

Doctor Emilia Palo
University of Turku
Turku, Finland

Reviewed by

Professor Kirsi Niinimäki
Aalto University
Espoo, Finland

Professor Mikko Mäkelä
VTT Technical Research Centre of Finland
Espoo, Finland

Opponent

Professor Riikka Räisänen
University of Helsinki
Helsinki, Finland

Cover Image: Mikael Nyberg, University of Turku

ISBN 978-952-02-0468-6 (PRINT)
ISBN 978-952-02-0469-3 (PDF)
ISSN 2736-9390 (Print)
ISSN 2736-9684 (Online)
Painosalama, Turku, Finland 2025

Mamusi

UNIVERSITY OF TURKU
Faculty of Technology
Department of Mechanical and Materials Engineering
Materials Engineering
ALICJA ŁAWRYNOWICZ: Multifunctional light-responsive textiles and their sustainable development
Doctoral Dissertation, 176 pp.
Doctoral Programme in Technology (DPT)
September 2025

ABSTRACT

Photoresponsive textiles are gaining increasing attention for their potential in health monitoring, resource conservation, and comfort-related applications. Unlike electronic smart textiles, they deliver responsive functions without circuitry, offering prospects of simpler fabrication and reduced environmental impact. This thesis investigates the potential of such non-electronic photoresponsive textiles through two case studies and a critical assessment of the field from a broader perspective.

The first part introduces hackmanite-coated textiles as ultraviolet (UV)-monitoring tools. For the first time, hackmanite was successfully deposited onto fabric using a safe and simple coating method. The resulting textiles displayed a strong UV-induced color change from white to purple, with a response threshold closely matching the erythemal action spectrum of human skin. This feature enabled accurate monitoring of UV index (UVI) values below 3, the level at which protective measures are recommended to prevent early sunburn. Furthermore, the fabric exhibited exceptional fatigue resistance, maintaining stable coloration over at least 20 photochromic cycles, confirming its potential as a reliable UV-sensing material.

The second part focuses on ZnO-coated photocatalytic textiles and the influence of synthesis parameters on their self-cleaning and UV-blocking performance. A systematic study of nine parameters identified conditions yielding flower-like ZnO morphologies with superior photocatalytic activity. The refined coatings exhibited nearly complete UV blocking and effective self-cleaning, achieving 73 % methylene blue (MB) degradation within 1 h and 90 % after 24 h of solar exposure, as well as 32 % removal of coffee stains after 1 h and 82 % after 24 h.

The final part presents a critical review of 130 peer-reviewed studies on photoresponsive non-electronic textiles, revealing significant gaps between laboratory demonstrations and real-world applicability. A key issue was that these textiles were frequently tested under high-intensity, single-wavelength light sources that are rarely achievable in everyday indoor or outdoor environments. As a result, many proposed applications remain unverified in their intended settings, and the suggested benefits claimed under such idealized conditions were often overly optimistic. Some health-related uses, such as UV monitoring and self-disinfecting fabrics, appear promising. However, in most cases, further research and life-cycle studies are required to evaluate usability under intended lighting conditions and to validate sustainability claims.

KEYWORDS: smart textiles; photoresponsive textiles; sun-activated textiles; light-responsive; sustainability; photochromic; photocatalytic; self-cleaning; UV blocking; UV sensing

TURUN YLIOPISTO
Teknillinen Tiedekunta
Kone- ja Materiaalitekniikan Laitos
Materiaalitekniikka
ALICJA ŁAWRYNOWICZ: Multifunctional light-responsive textiles and their sustainable development
Väitöskirja, 176 s.
Teknologian tohtoriohjelma (DPT)
Syyskuu 2025

TIIVISTELMÄ (IN FINNISH)

Kiinnostus valoon reagoivia tekstiilejä kohtaan kasvaa niiden terveyden seurantaan, resurssien säästämiseen ja mukavuuteen liittyvien sovellusten tarjoamien mahdollisuuksien vuoksi. Toisin kuin elektroniset älytekstiilit, nämä tekstiilit tarjoavat reagoivia toimintoja ilman virtapiirejä, mikä mahdollistaa yksinkertaisemman valmistuksen ja pienemmän ympäristövaikutuksen. Tämä väitöskirja tutkii tällaisten ei-elektronisten valoon reagoivien tekstiilien potentiaalia kahden tapaustutkimuksen, ja laajemmasta näkökulmasta alan kriittisen arvioinnin avulla.

Ensimmäisessä osassa esitellään hackmaniitilla päällystetyt tekstiilit UV-säteilyn seurantatyökaluina. Hackmaniittia onnistuttiin ensimmäistä kertaa yhdistämään kankaaseen turvallisella ja yksinkertaisella päällystysmenetelmällä. Tuloksena saadut tekstiilit osoittivat voimakasta UV-valon aiheuttamaa värimuutosta valkoisesta violetiksi, jonka vastekynnys vastasi hyvin ihmisen ihon punoitusta aiheuttavaa spektriä. Ominaisuus mahdollisti luotettavan seurannan UV-indeksiarvoille alle 3, jolloin suojatoimenpiteitä suositellaan varhaisten auringonpolttamien välttämiseksi. Sen lisäksi kangas osoitti erinomaista väsymiskestävyyttä säilyttäen päällysteen värin vakaana yli 20 fotokromisen syklin ajan, mikä vahvistaa sen potentiaalin luotettavana UV-säteilyä havaitsevana materiaalina.

Toinen osa keskittyy sinkkioksidilla (ZnO) päällystettyihin fotokatalyyttisiin tekstiileihin sekä synteesiparametrien vaikutukseen niiden itsepuhdistumiseen ja UV-säteilyn estokykyyn. Yhdeksän parametrin systemaattinen tutkimus tunnisti olosuhteet, joissa syntyi kukanmuotoisia ZnO-morfologioita, joilla oli erinomainen fotokatalyyttinen aktiivisuus. Optimoidut pinnoitteet saavuttivat lähes täydellisen UV-säteilyn eston ja tehokkaan itsepuhdistuvuuden: metyleenisinisen hajoaminen oli 73 % yhden tunnin ja 90 % vuorokauden auringonvalolle altistuksen jälkeen. Kahvitahroista poistui tunnissa 32 % ja 24 tunnissa 82 %.

Viimeinen osa esittelee kriittisen katsauksen 130 vertaisarvioituun tutkimukseen valoon reagoivista ei-elektronisista tekstiileistä paljastaen merkittäviä eroja laboratoriotestien ja todellisen soveltuvuuden välillä. Keskeinen ongelma oli, että näitä tekstiilejä testattiin usein voimakkailla, yhden aallonpituuden valonlähteillä, joita harvoin esiintyy tavallisissa sisä- tai ulkotiloissa. Tämän seurauksena näiden monet ehdotetut sovellukset ovat edelleen vahvistamattomia niiden aioituissa ympäristöissä, ja tällaisiin ideaalisiin olosuhteisiin perustuvat väitteet hyödyistä olivat usein liian optimistisia. Jotkin terveyteen liittyvät sovellukset, kuten UV-säteilyn valvonta ja itsedesinfioituvat kankaat vaikuttavat lupaavilta. Useimmissa tapauksissa tarvitaan kuitenkin lisätutkimusta arvioimaan käytettävyyttä todellisissa valaistusolosuhteissa, sekä elinkaaritutkimusta kestävyysväitteiden vahvistamiseksi.

ASIASANAT: älykkäät tekstiilit, valoon reagoivat tekstiilit, auringonvalolla aktivoituvat tekstiilit, valoon reagoiva, kestävyys, fotokrominen, fotokatalyyttinen, itsepuhdistuva, UV-suojaava, UV-havaitseva

Table of Contents

Abbreviations

AS/NZS	Australian / New Zealand Standard
BBP	Benzyl Butyl Phthalate
CIE	International Commission on Illumination (fr. Commission Internationale de l'Éclairage)
CNTs	Carbon nanotubes
CO2	Carbon Dioxide
DI H2O	Deionized water
DINCH	Di(isononyl)cyclohexane-1,2-dicarboxylate
Ebg	Band gap
EN	Euronorm (European Standards)
FE-SEM	Field emission scanning electron microscope
g-C3N4	Graphitic Carbon Nitride
GO	Graphene oxide
HVAC	Heating, ventilation, and air conditioning
IR	Infrared
ISO	International Organization for Standardization
MB	Methylene Blue
MgO	Magnesium Oxide
NaOH	Sodium Hydroxide
NH_4OH	Ammonium Hydroxide
NIR	Near-infrared
NPs	Nanoparticles
PAzo	Azobenzene-containing polymer
PCMs	Phase-change materials
PDA	Polydopamine
PDF	Powder Diffraction File™
PVB	Polyvinyl Butyral
RGB	Red, green, blue
RH	Relative humidity
Tg	Glass transition temperature
TiO2	Titanium Dioxide

UPF	Ultraviolet Protection Factor
UV	Ultraviolet
UVI	Ultraviolet Index
VIS	Visible
WO_3	Tungsten Trioxide
XRD	X-ray powder diffraction
ZnAc	Zinc Acetate Dihydrate
ZnO	Zinc Oxide

List of Original Publications

This dissertation is based on the following original publications, which are referred to in the text by their Roman numerals:

I **Lawrynowicz, A.**, Vuori, S., Palo, E., Winther, M., Lastusaari, M., Miettunen, K. Transforming fabrics into UV-sensing wearables: A photochromic hackmanite coating for repeatable detection, *Chem. Eng. J.*, 2024; 494: 153069.

II **Lawrynowicz, A.**, Palo, E., Nizamov, R., Miettunen, K. Self-cleaning and UV-blocking cotton – Fabricating effective ZnO structures for photocatalysis, J. *Photochem. Photobiol. Chem*., 2024; 450: 115420.

III **Lawrynowicz, A.**, Palo, E., Vapaavuori, J., Bang, A.L., Dumitrescu, D., Miettunen, K. From Laboratory to Reality: Critical Analysis of Light-Activated Non-Electronic Smart Textiles and Their Claimed Benefits. *Manuscript submitted.*

List of related publications not included in the thesis

Miettunen, K., Hadadian, M., García, J.V., **Lawrynowicz, A.**, Akulenko, E., Rojas, O.J., Hummel, M., Vapaavuori, J. Bio-based materials for solar cells, *WIREs Energy Environ*., 2024; 13: e508.

Author's Contribution

The author was mainly responsible for all parts of Publications I–III (i.e., Conceptualization, Methodology, Formal Analysis, Investigation, Data Curation, Validation, Writing—Original Draft, Visualization). Besides supervision and Writing-Editing, the other key contributions by collaborators were as follows: **Dr. Emilia Palo** (Publications I–III) contributed to the writing process and data analysis, particularly in Publication II (i.e., Formal analysis and Visualization in sections describing XRD analysis and the explanation of ZnO crystal formation) and in Publication III (i.e., Investigation and Methodology in the primary analysis). **Prof. Mika Lastusaari** (Publication I) originated the concept of using hackmanite mineral as a UV-sensing material. **Dr. Sami Vuori** (Publication I) provided the original coating recipe, contributed to the writing of the original draft (sections describing the crystal structure of hackmanite and its photochromic properties), assisted with the preparation of experimental work (coating formulation), and contributed to the formal analysis of reflectance spectra in color-changing experiments. **Rustem Nizamov** (Publication II) contributed by analyzing images taken during the self-cleaning tests and writing the corresponding methods section. **Mathias Winther** (Publication I) contributed to the setup preparation for durability tests (washing and bending).

In addition, artificial intelligence (AI) tools such as ChatGPT, Grammarly, and Claude.AI were used to improve the language of this thesis, by correcting grammar, identifying misspellings, and enhancing readability. In addition, Figure 3 in Publication III (i.e., Figure 17 in this thesis) was created with the help of Leonardo.AI. AI was not employed in the development of research concepts, data analysis, or the formulation of conclusions.

1 Introduction

The aim of this thesis was to develop multifunctional photoresponsive smart textiles and critically assess their potential to deliver recognised social and environmental benefits (*Figure 1*). Smart textiles have gained increasing research attention due to their ability to respond not only to electrical stimuli but also to light, heat, and mechanical pressure, thereby extending the traditional role of fabrics with new functionalities.[1–5] The most established category, electronic textiles (e-textiles), incorporates electrical circuits into the fabric structure, enabling a wide range of interesting applications.[1,6] Examples include continuous health monitoring, particularly valuable for elderly or chronically ill individuals,[7] energy generation, which can support use in remote conditions,[8] and data transmission, allowing, for example, contactless payments.[9]

However, despite these exciting possibilities, their wider adoption remains constrained by performance limitations, scalability issues, and high production costs.[10] It should be noted that integrating electronics into fabrics introduces significant operational and sustainability challenges.[11–13] Electrical components are susceptible to moisture, mechanical stress, and repeated laundering, which greatly shortens their lifespan.[5,14] Their maintenance can be demanding, and the failure of a single component may disable the entire system.[12] Furthermore, since they contain embedded electronics, e-textiles are classified as electronic waste rather than conventional textiles, complicating their end-of-life processing and posing serious barriers to circular management.[15] Consequently, many e-textiles continue to be regarded as niche or even extravagant gadgets, rather than life-enhancing technologies capable of meeting consumer needs.[10]

These limitations point to the need for alternative approaches that remove electronic components from smart textiles while retaining their desired stimulus-responsive functionality. Photoresponsive textiles offer a particularly compelling solution, since they can directly harness energy from light (e.g., sunlight) to provide functions like self-cleaning, color changing, and heat generation.[16–18] These properties can be achieved through relatively simple surface modifications of conventional fabrics, allowing production at lower cost and with greater ease than electronic alternatives. By utilizing light as the primary energy source, photoresponsive textiles remain operational wherever sufficient illumination is available.[12] This self-

sustaining mechanism makes them particularly promising for applications in regions with limited access to reliable electricity or healthcare infrastructure, where they could provide valuable functions such as UV-monitoring or self-disinfection, without requiring complex or energy-intensive support systems.[19]

Moreover, the absence of electrical components potentially allows these textiles to maintain the flexibility, softness, and ease of care typical of conventional fabrics, while still delivering advanced functionality. Without circuits, they are often easier to wash, less prone to damage, and simpler to maintain than their electronic counterparts.[5] End-of-life processing is possibly more straightforward, since there are no electronic parts to remove before recycling.[20] Given that sunlight is an abundant and renewable energy source, photoresponsive textiles could be strategically valuable for sustainable development.[19]

With these advantages, photoresponsive textiles are increasingly explored for applications in healthcare, resource conservation, and comfort enhancement, often with smaller environmental footprints than conventional solutions. Color-changing textiles, for example, can function as UV-sensing devices, alerting wearers to excessive sun exposure and helping reduce the risk of sunburn and related health complications.[21–23] Self-cleaning fabrics could decrease laundering frequency, thereby reducing water consumption and minimizing the release of detergents into aquatic environments.[24–26] Conveniently, many textiles are commonly used in light-exposed environments, such as outdoors in boats, sails, outdoor furniture, and tents, and indoors in curtains, furniture, and clothing, making them well-positioned to utilize available sunlight effectively.[12]

The purpose of this thesis was to develop and characterise photoresponsive textiles with two distinct functionalities, photochromic (color-changing; **Publication I**) and photocatalytic (self-cleaning and UV-blocking; **Publication II**) properties. The photochromic textiles were fabricated using the mineral hackmanite, which was successfully coated onto a textile substrate for the first time (**Publication I**). The main objective of this work was to obtain a reliable wearable capable of monitoring UVI levels and alerting users to excessive UV exposure to enable preventive measures. For **Publication II**, the photocatalytic textiles were produced through the in-situ coating of ZnO on cotton. This part of the study aimed to achieve an effective self-cleaning and UV-blocking textile surface while establishing a reproducible synthesis protocol of flower-like ZnO crystal structures.

In addition to the experimental work, this thesis presents a critical analysis of non-electronic photoresponsive textiles as a broader category (**Publication III**; see *Figure 1*). The goal was to evaluate whether the functionalities often claimed in recent literature can be realised, for example, under intended lighting conditions. This discussion is grounded in the review of 130 peer-reviewed studies and complemented by the results from Publications I and II. Finally, this thesis provides a comprehensive perspective on the feasibility of photoresponsive textiles, offering

guidance for future developments that prioritises delivering realistic benefits while minimising unintended negative consequences. The work is based on the three original publications listed on page 10.

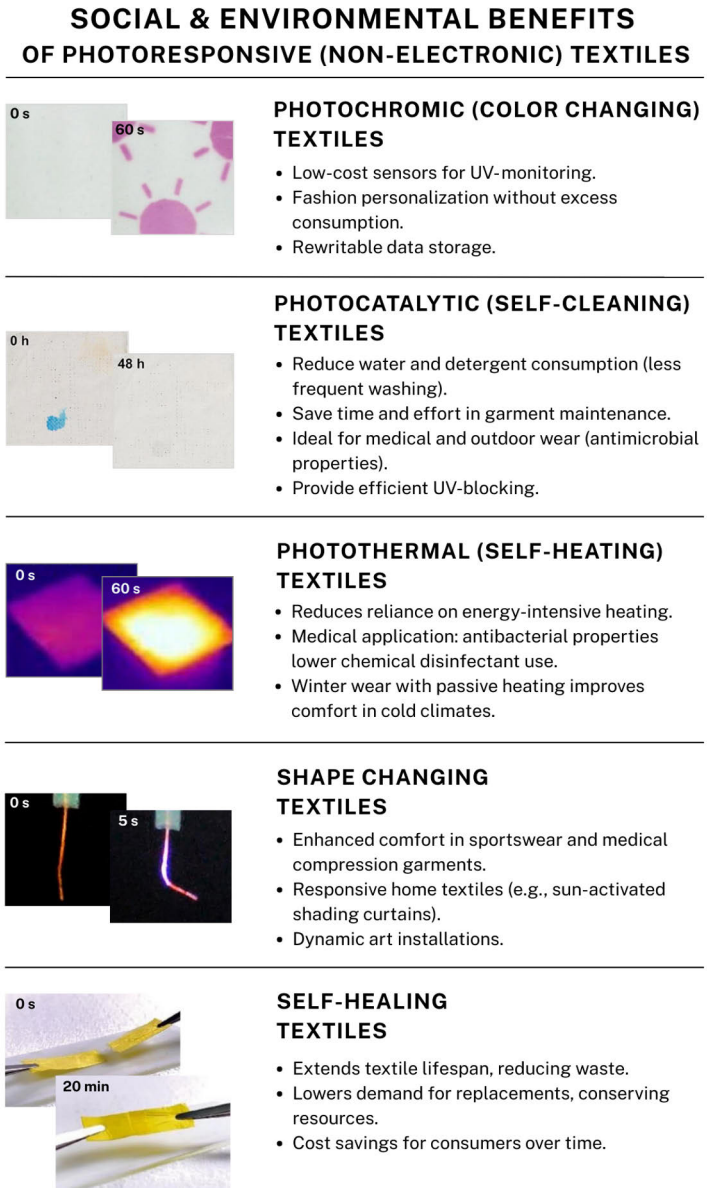

Figure 1. Photoresponsive smart textiles can be classified according to their response to light, including photochromic (color-changing), photocatalytic (self-cleaning), photothermal (self-heating), shape-changing, and self-healing systems. Their potential applications, summarized here based on the comprehensive review presented in **Publication III**, highlight both environmental and social benefits. Permissions for the use of these icons are provided separately under the images in this thesis.

2 Literature Review

The literature review provides the scientific foundation for this work and is structured into three main parts. First, it discusses various methods for integrating light-responsive particles into textiles, with particular focus on the coating methods applied in this thesis. Second, it presents an overview of photoresponsive textiles, with an emphasis on photochromic and photocatalytic features, which are central to this study (**Publications I** and **II**). Other categories, such as photothermal, shape-changing, and self-healing textiles, are covered more briefly to provide a broader context in this thesis, particularly for **Publication III**. These features are discussed in terms of their photoresponsive working mechanisms, material choices, and potential applications. Lastly, this section offers a background on practical applications of photoresponsive textiles, highlighting the gap between their theoretical benefits and real-world performance.

2.1 Methods for integrating light-responsive particles into textiles

Photoresponsive compounds can be incorporated into textiles through several techniques, each with distinct benefits and limitations.[27] The primary approaches include embedding functional materials within yarns or applying them as coatings to fabric surfaces. The first route involves introducing light-active particles directly into fibers by dispersing them in a polymer melt or solution prior to fiber formation, using techniques such as melt,[28] wet,[29] and electrospinning[30] (*Figure 2A*). Integrating particles within the fiber structure creates a protective microenvironment that shields them from abrasion, UV radiation, and environmental degradation. Using spinning methods is generally known for improving retention during repeated laundering and extend functional stability, although the durability depends largely on the mechanical integrity of the fibers.[31]

For example, high particle loadings, (e.g., 5–10 wt %), can disrupt polymer chain orientation, reduce crystallinity, and lower tensile strength and elasticity of functionalised yarns.[21,32] Moreover, locating particles deep within the fibers core limits light penetration and reduces accessible surface area, which can weaken the photoresponsive effect.[12,33] Fang *et al.*[21] demonstrated these effects by

incorporating the photochromic mineral hackmanite into cellulose-based Ioncell yarns via wet spinning. Increasing the hackmanite content from 2 to 10 wt % improved the coloration change but reduced fiber tenacity and elongation from 50 to 35–40 cN/dtex (50 % relative humidity; RH). An optimal loading of 3.5 % preserved mechanical performance for 18,000 abrasion cycles and 2,000 pilling cycles, although the reduced content limited the photochromic response.[21]

These limitations become more problematic when functional yarns are blended with non-functional fibers or positioned beneath the garment surface.[12] In such cases, surrounding fibers can scatter or absorb light, reducing the exposure of photoresponsive particles and diminishing their effect. Their production can also be challenging, especially when particle dispersion is uneven or the active material content is high. Poor dispersion often leads to particle agglomeration, which increases surface roughness and can introduce structural flaws such as spinning defects or voids.[21,32] These flaws may weaken the yarn and make it harder to achieve consistent performance, which in turn can complicate large-scale manufacturing.

For photoresponsive wearables to become commercially viable, they must be simple to manufacture, cost-effective, and compatible with existing production methods.[34] One approach that can meet these criteria is the direct application of functional materials onto textile substrates through coating. Common techniques include dip-coating,[35,36] spray-coating,[37] and screen-printing[38] (*Figure 2B*). Other established methods, such as doctor blade coating and inkjet printing, enable the deposition of material with high spatial precision.[39,40] Among these techniques, the doctor blade method was chosen in **Publication I** for the experimental work, owing to its straightforward use and minimal equipment requirements.[41]

A key advantage of using coating instead of spinning methods is the ability to use pre-fabricated textile substrates (e.g., ready garments), which lowers manufacturing costs and supports scalability.[12] Since the deposited particles remain at or near the textile surface, they retain sufficient light accessibility. As a result, functionalities such as photochromic color change or photocatalytic processes are typically more efficient than in systems where the active particles are embedded deep within the fiber.[12] The drawback is that surface-exposed particles are more susceptible to abrasion and mechanical wear, which can lead to gradual loss of active material or, in some cases, coating delamination during normal use and laundering.[42] Additionally, exposure to detergents, UV light, and environmental pollutants can cause chemical degradation, particularly in organic compounds (see Section *2.2.1* for more details).

Strong adhesion between the coating and the textile substrate depends on factors such as fiber surface energy, residual processing chemicals, and any pre-treatment applied. For example, many synthetic textiles, such as polyester and elastane, have hydrophobic surfaces with limited chemical reactivity, resulting in weak adhesion.[43]

In contrast, cellulose-based substrates like cotton are naturally hydrophilic, and their ability to form hydrogen bonds enhances particle adhesion.[44–46] Surface pre-treatments (e.g., plasma treatment or corona discharge) can increase surface energy and improve bonding,[43,47] although these techniques add complexity and cost to the manufacturing process. Post-treatments like heat-setting, commonly used in screen printing, can also improve adhesion between a functional coating (e.g., color-changing print) and the substrate.[48] However, elevated temperatures may degrade thermally sensitive particles and compromise their photoresponsive performance.

An additional strategy to improve coating durability is encapsulating the photoresponsive particles within protective shells made of materials such as thermoplastic polyurethane,[49] poly(methyl methacrylate),[50] chitosan,[51,52] or silica[53]. Encapsulation can improve interfacial adhesion, enhance wash fastness, and increase mechanical durability by shielding the active particles from moisture, oxygen, and chemical degradation.[54] For photochromic materials, the encapsulating layer must remain optically transparent to allow sufficient light transmission and ensure accurate color responsiveness, as shown in numerous studies.[55] In contrast, photocatalytic particles such as TiO_2 and ZnO require direct exposure to both light and the surrounding environment to carry out surface redox reactions. For these materials, full encapsulation can block reactive sites and significantly reduce photocatalytic activity.[56]

A specialized category of surface treatment involves the direct in-situ growth of active crystals on intended substrates. Since in-situ techniques enable controlled particle formation, they are particularly advantageous for applying nanoparticles (NPs) on textiles. Such methods allow precise control over crystal morphology (a parameter that strongly influences NPs performance; see Section *2.3.1*), while also improving dispersion and adhesion to the substrate.[57] Common in-situ techniques include chemical bath deposition,[58] variations of hydrothermal treatment,[59–61] and related processes[27]. Among these methods, microwave-assisted synthesis has gained particular attention for its rapid processing, energy efficiency, and cost-effectiveness compared to conventional hydrothermal processes.[62–66] For these reasons, microwave-assisted synthesis was employed as the synthesis route in **Publication II**.

The choice of integration method is generally guided by factors such as functional requirements, target applications, scalability potential, and available infrastructure. For example, the required amount and distribution of photoactive materials depend strongly on the intended use. UV-sensing textiles often require only localized deposition, whereas self-cleaning applications generally demand full-surface coverage. In self-healing textiles, active compounds are usually embedded within fibers to enable a bulk response, unless they are added to surface coatings to improve durability. For photothermal textiles, coverage requirements vary. A small section of photoresponsive yarn may be sufficient to provide thermal comfort, while thermal self-disinfection requires treatment across the entire fabric. Selecting an

application-specific strategy, therefore, helps optimise performance while minimising material use and production costs, and this principle was applied throughout the experimental work presented in this thesis.

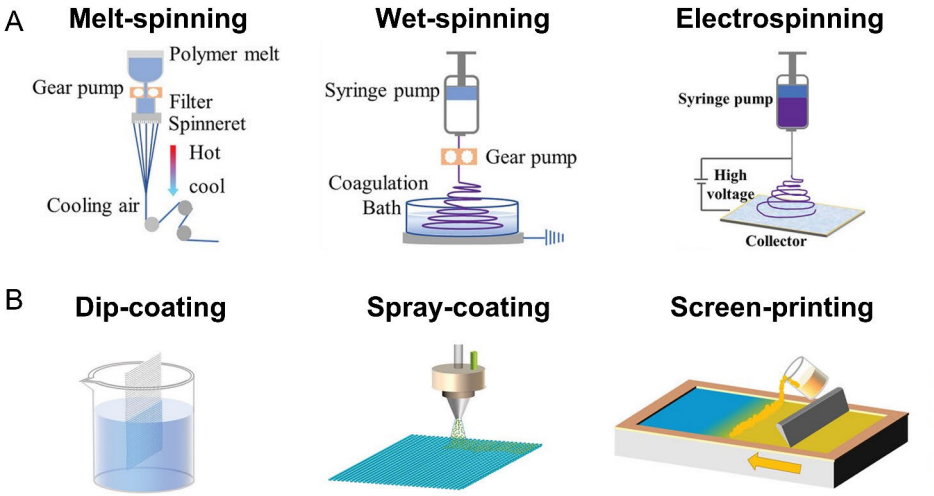

Figure 2. Schematic of functional textile fabrication using various **(A)** spinning methods (*from left to right*): melt-spinning, wet-spinning, and electrospinning, **(B)** coating methods (*from left to right*): dip-coating, spray-coating, and screen-printing. Adapted with permission.[27] Copyright 2023, Wiley-VCH GmbH.

2.2 Photochromic textiles

The first category of photoresponsive textiles discussed in this thesis is photochromic textiles, which are of particular relevance here due to their promising potential in health-related applications (see *Figure 1*). These materials are a class of smart textiles capable of reversible color changes when exposed to specific wavelengths of light, most often in the UV range.[67] Generally, the color transformation is driven by intrinsic chemical properties of the embedded photochromic compounds. For example, textiles containing azobenzene compounds can shift from yellow to orange (*Figure 3A*),[68] those with spiropyran turn from colorless to purple (*Figure 3B*),[23] while hackmanite minerals shift from white to purple (*Figure 3C*)[21,69]. These materials can be broadly divided into two groups, organic molecules (e.g., spiropyrans, spirooxazines, and azobenzenes) and inorganic materials (e.g., WO_3 and hackmanites).[70] Each group operates through distinct photoactivation mechanisms, which in turn influence key performance parameters such as color stability, fatigue resistance, and environmental durability. These factors determine their suitability for various applications, including UV sensors, information storage, and decorative (e.g., fun) or aesthetic uses.[17,21,71,72]

2.2.1 Photochromic materials and their functional performance

The first category, organic photochromic materials, is valued for its vibrant, tunable color responses and broad commercial availability.[73] These compounds change color through photoreactions in their functional groups, most commonly via isomerization between two distinct structural forms (e.g., spiropyran ↔ merocyanine).[55,74–76] Reversion to the original state typically occurs through thermal relaxation or secondary photoexcitation, depending on the specific molecular or system design.[74,77]

Despite their attractive optical properties, organic photochromic materials often experience photochemical fatigue after repeated switching cycles, which can limit their suitability for applications requiring high durability.[54,78] Since many of these compounds contain reactive unsaturated bonds, they are susceptible to environmental factors such as pH, oxygen, and solvent polarity.[51,52,74,79] These vulnerabilities further contribute to limited photostability during prolonged UV exposure, as repeated excitation accelerates irreversible bond cleavage or oxidation. For example, spiropyran-based fabrics showed a progressive loss of saturation after only 10 photochromic cycles in two independent studies.[23,80] Moreover, several commonly used organic photochromic compounds (e.g., azo-based remazol red and disperse red dyes) have been reported to pose ecological risks, particularly when released into aquatic environments.[81–83] Their use in textiles should therefore be carefully evaluated for environmental safety, especially in scenarios where leaching during washing or degradation may occur.

In contrast to their organic counterparts, the second category of photochromic materials (i.e., inorganic minerals), exhibits a more limited range of color changes but offers superior resistance to UV degradation and environmental wear. Inorganic photochromism typically arises from photoinduced electron transfer or defect formation within a crystalline lattice.[84] In the case of hackmanite ($Na_8Al_6Si_6O_{24}(Cl,S)_2$), focus of **Publication I**, structural rigidity of the mineral itself protects the underlying electronic transitions, resulting in enhanced photostability (*Figure 3C*).[69,85] The reversion to the original color state occurs through visible (VIS) light exposure or mild thermal treatment.[86] Since the switching process in hackmanite involves no irreversible chemical changes at the atomic level, color recovery does not require overcoming significant energy barriers, maintaining their color saturation over multiple photochromic cycles. These minerals have been reported to preserve color intensity for at least 13 cycles without notable loss of saturation, and their stability is expected to extend over many more, supporting their use in durable textile-based UV sensors.[69,85]

Moreover, recent studies on hackmanites have broadened the color range traditionally associated with these minerals, which were often limited to pink or purple tones. By modifying synthesis protocols, alternative photochromic responses have been achieved, such as yellow or blue coloration under UV light,[87] thereby

expanding design flexibility. Hackmanites are also regarded as environmentally benign, offering a safer option in situations where material release into natural ecosystems may occur, making them well-suited for wearable applications.[67]

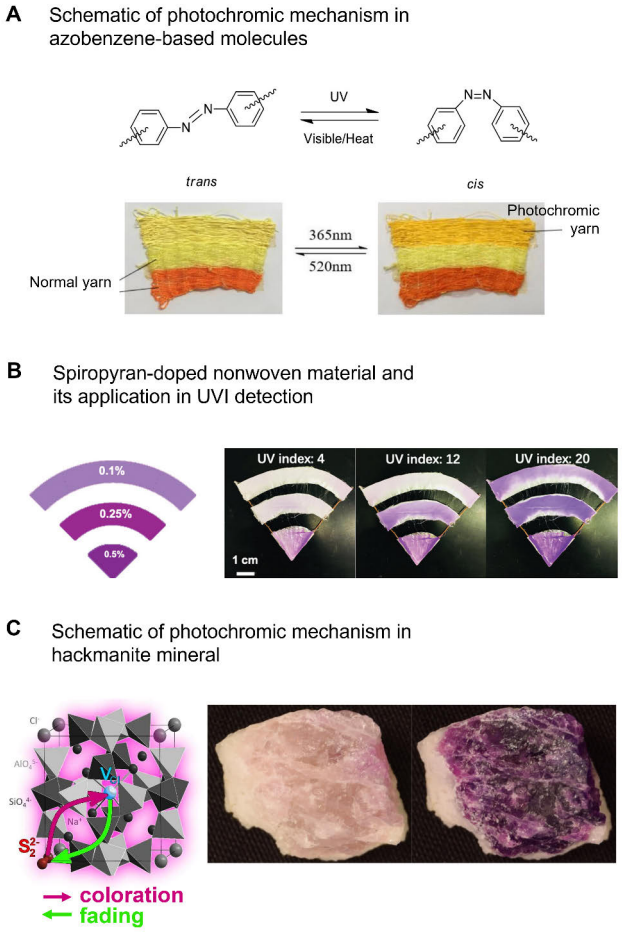

Figure 3. **(A)** Photochromic mechanisms azobenzene-loaded textiles; Azo-derivative undergoing reversible trans–cis isomerization (*top)* and a knitted fabric example incorporating the photochromic material (P6ABE@PVDF) alongside commercial yarns (*bottom*). Adapted with permission.[68] Copyright 2022, Elsevier B.V. **(B)** "Wi-Fi" icon as a UV sensor; schematic showing color change intensity corresponding to different spiropyran concentrations in each beam (*left*) and a photo of the electrospun polycaprolactone fibers doped with spiropyran dyes forming the icon, exposed to UV irradiation at UVI 4, 12, and 20 for 5 s (*right*). Adapted with permission.[23] Copyright 2020, Wiley-VCH GmbH. **(C)** Schematic illustration of the hackmanite unit cell showing electron trapping (purple arrow) and detrapping (green arrow) under proper wavelengths; in hackmanite, the disulfide ion (S_2^{2-}) absorbs UV light and transfers an electron to a chlorine vacancy V_{cl}, creating a color center that absorbs around 530 nm, causing the characteristic purple color of hackmanites (*left*). **Publication I**; Adapted under terms of the CC-BY license.[22] Copyright 2024, The Authors, published by Elsevier B.V.; Photos of hackmanite mineral in its colorless and colored form (*right*). Adapted under terms of the CC BY-NC-ND license.[69] Copyright 2022, the Authors, published by PNAS.

2.2.2 Applications in UV detection and protective textiles

The reversible color-changing behavior of photochromic materials presents opportunities not only in adaptive fashion, identity expression, and interactive design,[17,88] but also in mitigating the environmental footprint of the textile sector. By enabling tunable coloration within a single garment, these materials can reduce the demand for multiple clothing items, thereby decreasing overall textile consumption and its associated emissions.[89]

Perhaps more importantly, in certain materials, such as hackmanites or spirooxazines, color saturation correlates directly with radiation intensity, making them particularly attractive for UV-sensing applications.[23,70] This feature allows for the development of textiles that act as real-time UV dosimeters, providing immediate visual feedback when UV levels exceed safe exposure thresholds. Such garments could prompt users to seek shade, apply sunscreen, or take other protective measures before sunburn occurs. The potential health impact is substantial, since 65–90 % of melanoma cases, the most lethal form of skin cancer, are linked to excessive UV exposure.[90,91] In alone Finland more than 1700 people are diagnosed with melanoma and about 200 die from melanoma each year.[92] Chronic UV exposure is also associated with other conditions, such as actinic keratosis, basal and squamous cell carcinomas, and ocular damage,[93,94] many of which could be prevented through improved sun-protective behaviors. Clinical studies have reported that measures such as avoiding midday sun, using sunscreen, and wearing protective clothing significantly reduce the risk of sunburn and related diseases.[91,93] However, individuals are often unaware when they are at high risk.[94] For instance, melanoma incidence is paradoxically higher in Northern Europe than in Mediterranean regions, despite lower UVI values, likely due to a combination of genetic susceptibility and insufficient sun-protection behaviors.[95] These findings highlight the potential of real-time UV-monitoring garments to support more effective and personalized sun-protective strategies.

The chromatic response of photochromic materials can be calibrated to indicate either cumulative UV dose (J m^{-2}) or real-time UVI values.[23,96] While cumulative UV dose provides a general measure of total exposure, the UVI (established by the World Health Organization) defines standardized risk categories for short-term exposure. UVI monitoring primarily assesses outdoor UV irradiation and its correlation with the erythemal action spectrum. UVI values of 0–2 indicate low risk, 3–5 moderate, 6–7 high, and ≥ 8 very high to extreme, requiring rigorous protective measures.[97]

The challenge is that UV radiation fluctuates throughout the day and across locations, while standard UVI forecasts average data over large areas, overlooking local variations that affect individual exposure.[97,98] Continuous, localized UV monitoring can therefore provide more accurate data, making it a practical application for UV-responsive textiles. Synthetic hackmanites are particularly suitable for this purpose, since their color change threshold aligns closely with the

erythemal action spectrum.[70] Notably, before this work, hackmanite had never been applied to textiles using conventional coating methods. The only earlier example, by Fang *et al.*,[21] embedded hackmanite into cellulose-based yarn via wet-spinning—a method restricted to specific manufacturing routes and incompatible with commercial fabrics. Moreover, the resulting yarn responded only to UV-C radiation, which is absorbed by the atmosphere and does not reach the Earth's surface.[70] This thesis addresses these limitations by applying hackmanite as a textile coating, achieving for the first time a UV-A/B–responsive hackmanite-enriched fabric and establishing a practical route for its use in UV-monitoring applications.

2.3 Self-cleaning (photocatalytic) textiles

Photocatalytic textiles form another important group of photoresponsive textiles due to their broad range of applications in both health and environmental fields (see *Figure 1*). By incorporating semiconductor particles (often in NP form), such as TiO_2, ZnO, and g-C_3N_4 into textiles, these materials achieve dual functionality as both self-cleaning and UV-blocking fabrics.[99–102] When exposed to light, photocatalytic textiles degrade organic pollutants on their surfaces through oxidative processes, while absorbing hazardous UV (*Figure 4*).

The self-cleaning process begins when the photocatalytic material absorbs photons with energy equivalent to or exceeding the photocatalyst's band gap. This energy is sufficient to excite electrons from the valence band to the conduction band while leaving holes behind, thus forming electron-hole pairs (*Figure 4A*). Three pathways exist for these photogenerated pairs: (1) rapid recombination of electron-hole pairs either on the surface or within the bulk of the photocatalyst, (2) photoreduction, where electrons (e^-) interact with oxygen molecules in air, generating superoxide anion radicals ($\bullet O_2^-$) on the material surface, and (3) photooxidation, where positive holes (h^+) oxidize water molecules present in ambient humidity, generating highly oxidizing hydroxyl radicals (•OH). The resulting reactive oxygen species decompose organic contaminants adhered to the material surface, including dyes, oils, and microbes, converting them into harmless byproducts such as CO_2 and H_2O (*Figure 4B*).[103,104]

Ideally, the self-cleaning function should operate automatically during regular wear with minimal user effort and just be accelerated under direct light exposure. However, photocatalytic efficiency depends critically on factors such as material properties (particularly optical characteristics), particle size, light wavelength, and exposure duration, which can make efficient photocatalytic textiles challenging to fabricate.[27] For example, the optical absorption of photocatalytic materials is determined by their bandgaps (E_{bg}). Anatase TiO_2 ($E_{bg} \approx 3.2$ eV) absorbs UV light below 387 nm, and ZnO ($E_{bg} \approx 3.3$ eV) below 380 nm, restricting their activity to UV-rich conditions. Cadmium sulfide ($E_{bg} \approx 2.4$ eV) responds to visible light up to

516 nm.[105–108] Bandgap tuning through doping (e.g., W-doped TiO_2) or heterojunctions (e.g., g-C_3N_4–TiO_2) can shift absorption toward longer wavelengths, enhancing visible-light activity and offering a viable route to high photocatalytic efficiency under realistic lighting.[109–111] Notably, the wide bandgaps ($E_{bg} > 3.0$ eV) provide excellent UV-blocking properties.[105,112] As a result, textiles treated with these particles can combine self-cleaning functionality with high-level UV protection, which is an especially valuable feature for garments intended for prolonged outdoor use, where sustained exposure to sunlight is needed to maximize photocatalytic efficiency (see Section *2.3.2* for more details).

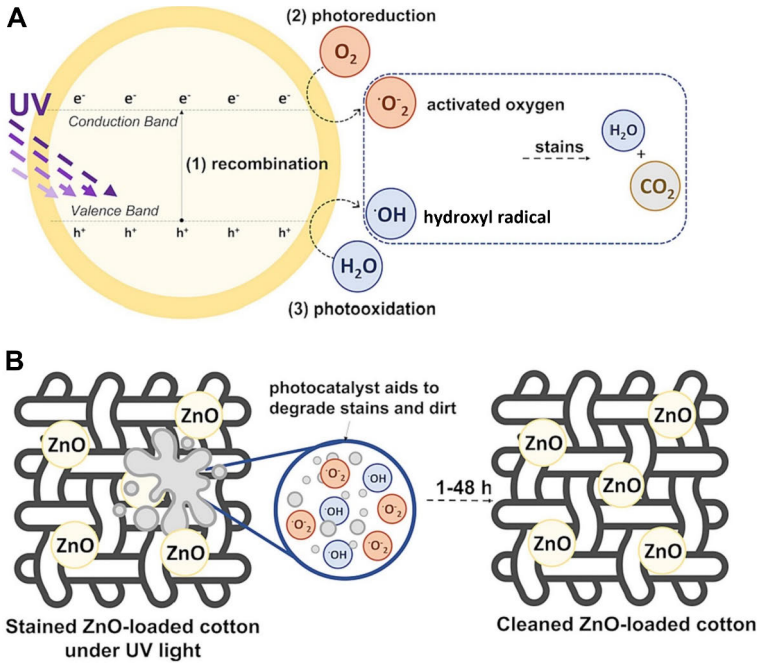

Figure 4. Schematic illustrations of **(A)** photocatalytic activity of ZnO when exposed to UV, **(B)** photocatalytic self-cleaning process appearing on ZnO-coated textile surface. **Publication II**; Adapted under terms of the CC-BY license.[24] Copyright 2023, The Authors, published by Elsevier B.V.

Some photocatalytic materials exhibit intrinsic antimicrobial activity that functions independently of light exposure, further enhancing self-cleaning.[113] For example, silver compounds (silver nanoparticles (AgNPs) or combined materials) demonstrate particularly strong dark-condition activity, with AgNPs penetrating pathogens while releasing atoms and ions that compromise cell membrane integrity [114]. Similarly, ZnO and hybrid materials such as TiO_2-ZnO maintain strong self-disinfecting capabilities regardless of lighting conditions,[100] while TiO_2 requires light for optimal performance.[99,101]

While TiO_2 remains the most widely used photocatalyst in commercial applications, ZnO has emerged as a promising alternative due to its exceptional physicochemical properties, including biocompatibility, high photostability, and low toxicity.[115–121] Several studies have demonstrated higher efficiency of ZnO over TiO_2 in generating photoactive species.[122] Additionally, ZnO structures arranged in thin layers offer greater flexibility than their TiO_2 counterparts.[123] For these reasons, ZnO may be considered a more suitable candidate for textile-based applications and was therefore selected for use in in **Publication II**.

2.3.1 Influence of ZnO morphologies on self-cleaning performance

The photocatalytic performance of ZnO is highly morphology-dependent, with properties varying significantly based on crystal size, shape, and surface coverage.[124] Consequently, not all ZnO crystal morphologies are suitable for highly efficient self-cleaning systems.[122] To optimize photocatalytic performance, studies have explored diverse ZnO nanostructures, including nanowires, nanorods, and flower-like morphologies, with the latter demonstrating superior photocatalytic activity compared to other configurations.[125–128,64] This enhanced performance is attributed to their elevated surface-to-volume ratio, which maximizes both interaction with pollutant molecules and light harvesting efficiency.[116,129,130]

Although flower-like ZnO structures can be synthesized through several in-situ routs, no single method has yet ensured their reliable (and repeatable) growth directly on textile substrates.[116] This limitation arises because synthesis parameters (e.g., temperature, precursor concentration, reaction time) critically influence ZnO morphology,[131] while the porous and chemically heterogeneous nature of textiles further complicates achieving uniform and controlled crystal growth.[132] Several studies have emphasised the need to understand these relationships to optimize the fabrication of ZnO nanostructures suitable for textile applications.[133] To address this gap, **Publication II** systematically examines nine synthesis parameters and their effect on ZnO morphology and photocatalytic efficiency on cotton substrates, offering one of the first comprehensive studies to establish a robust protocol for obtaining flower-like ZnO structures on textiles.

2.3.2 Applications in environmental and UV-protective textiles

Self-cleaning textiles are often highlighted for their potential to reduce resource consumption by minimizing washing frequency and eliminating detergent chemicals that cause water pollution.[134,135] However, the complete UV-triggered self-cleaning

process can require up to 48 h (or even days),[136–138] which limits practicality for daily-worn clothing but makes these materials well-suited for specialized applications. In environments where conventional laundering is impractical, such as space missions and military operations, photocatalytic textiles can maintain stringent sterility requirements over extended periods.[62,139,140] These materials could also work well on delicate fabrics (e.g., silk) or bulky textile products (e.g., furniture upholstery and curtains), which are laundered infrequently and often replaced when soiled rather than cleaned.[141,142]

Healthcare applications present particularly compelling opportunities for self-cleaning textiles. As detailed in Section *2.3*, photocatalytic materials can effectively reduce microbial contamination under various lighting conditions, and in some cases even in the absence of light. In other words, they can continuously degrade pathogens like bacteria and viruses on medical garment surfaces with minimal effort from users. Such textiles could provide supplementary sterilization in addition to conventional methods, reduce cross-contamination risks, and potentially extend the operational lifespan of personal protective equipment, thereby delivering additional environmental benefits.[143–145]

Even more relevant to the focus of this thesis, photocatalytic textiles with optimal particles distribution and fabric structure provide excellent UV-protection, as demonstrated by Ultraviolet Protection Factor (UPF) ratings that frequently exceed 50.[146] The UPF is defined as the ratio of average effective UV radiance (290–400 nm) on unprotected skin compared to fabric-protected skin, and is calculated according to standardized UPF methods (Australian/New Zealand Standard (AS/NZS) 4399:1996; Euronorm (EN) 13758-1:2001) using the formula presented in Equation *1*.[147,148]

$$UPF = \frac{\sum_{\lambda=290\ nm}^{\lambda=400\ nm} E(\lambda)\times S(\lambda)\times \Delta\lambda}{\sum_{\lambda=290\ nm}^{\lambda=400\ nm} E(\lambda)\times S(\lambda)\times T(\lambda)\times \Delta\lambda} \quad (1)$$

where $E(\lambda)$ is solar spectral irradiance, $S(\lambda)$ is the erythema action spectrum, $T(\lambda)$ is the spectral transmittance of the fabric at wavelength λ, and $\Delta\lambda$ is the wavelength (nm) interval of the measurements.

The UPF classification system categorizes UV protection levels in textiles, based on measured UPF values, as presented in Table *1*. Note that textiles achieving UPF values above 15 already provide "good protection", effectively shielding against UV-induced skin damage, including erythema and long-term photoaging effects. Photocatalytic textiles have been demonstrated to achieve UPF values exceeding 50, representing the highest level of UV protection. For specialized application, where UV protection is a priority (e.g., in geographical regions where UVI values often exceeds 7), the UV-blocking efficiency could be further enhanced though specific weave patterns and fiber morphologies that maximize light scattering.[12]

Table 1. UPF classification system. Standard AS/NZS 4399:1996. **Publication II**; Adapted under terms of the CC-BY license.[24] Copyright 2023, The Authors, published by Elsevier B.V.

UPF range	UVR protection category	Effective UVR transmission, %
15 – 24	good protection	6.7 to 4.2
25 – 39	very good protection	4.1 to 2.6
40 – 50+	excellent protection	≤ 2.5

2.4 Other photoresponsive features

While this doctoral research focuses on photochromic and photocatalytic textiles, other light-driven functionalities, such as photothermal, shape-changing, and self-healing effects, are briefly discussed here to provide context for **Publication III**.

2.4.1 Photothermal textiles

Photothermal textiles incorporate materials that convert absorbed light into heat, typically through nonradiative relaxation, allowing for controlled surface temperature changes.[149,150] Highly effective systems include melanin-like organic compounds, such as polydopamine (PDA), which can reach temperatures above 100 °C under solar exposure.[151–153] Carbon-based materials (e.g., graphene oxide (GO) and carbon nanotubes (CNTs)) are also widely used due to their broad-spectrum light absorption and high thermal conductivity.[8]

Phase-change materials (PCMs) form another broad and widely utilised class of thermally active substances, encompassing materials such as paraffin wax, hydrated salts, and fatty acid derivatives.[154] These materials absorb and store thermal energy by undergoing phase transitions, such as solid-to-liquid melting, in which heat is absorbed and then released during liquid-to-solid solidification.[49,155] To improve solar–thermal energy conversion and enable remote, selective control of the process, PCMs can be combined with light-absorbing components such as TiO_2 or azobenzene-based composites.[156–158] For example, azobenzene's reversible trans-cis photoisomerization provides wavelength-selective control. In this case, UV light can be used to harvest energy (pre-heating), while visible light triggers heat release, allowing tunable thermal regulation.[156,159]

The temperature range achievable by photothermal textiles largely determines their applications. Moderate heating (30–40 °C) is suitable for personal thermal management,[155] while rapid heating to ≥ 50 °C enables sufficient disinfection of medical textiles.[160–162] For example, one study[163] demonstrated a photothermal facemask of spun-bonded nonwoven fabric coated with copper sulfide compound, which reached 79.5–130.9 °C within 15 s of IR irradiation (500–2000 W cm^{-2}; *Figure 5A*). This temperature was sufficient to inactivate nearly all tested surface microorganisms,

including bacteria and viruses.[163] Moreover, textiles offer applications for energy savings purposes, for example, increasing air-conditioning setpoints by just 2 °C can reduce indoor cooling energy use by over 20 %.[157] By regulating body temperature locally, widespread adoption of photothermal textiles could help lower global energy demand and, on a broader scale, contribute to climate change mitigation.[155]

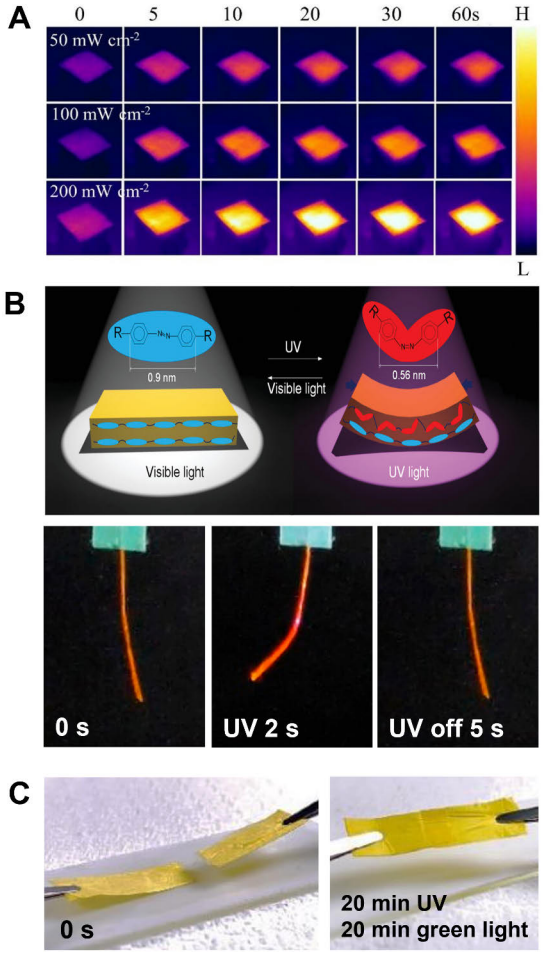

Figure 5. **(A)** Infrared image showing photothermal heating of a photothermal sample under different IR irradiances. Adapted with permission.[160] Copyright 2022, Elsevier B.V. **(B)** Trans–cis photoisomerization of azobenzene in liquid crystal polymers (*top*). Adapted with permission.[164] Copyright 2019, WILEY-VCH Verlag GmbH & Co. KGaA, Weinheim; Photomechanical response of covalent adaptable liquid crystal networks film (60 µm), where UV light (365 nm, 50 mW cm^{-2}) induces bending of the remolded film (*bottom*). Adapted with permission.[165] Copyright 2021, American Chemical Society. **(C)** Self-healing process of electrospun polystyrene and PAzo blend fibers. Self-healing occurs through photoisomerization of PAzo, which alters the glass transition temperature (T_g). Under UV light, T_g decreases, enabling bond exchange within the polymer matrix; subsequent exposure to green light re-solidifies the material. Adapted under terms of the CC-BY 4.0 license.[30] Copyright 2024, The Authors. Published by American Chemical Society.

2.4.2 Shape changing textiles

Light-responsive shape-changing textiles are dynamic materials capable of reversible bending, contraction, or expansion upon exposure to light. These transformations arise from photothermal or photochemical processes mediated by photoresponsive compounds embedded within the polymer matrix. Photothermal agents such as GO[166] or PDA[167] absorb light and convert it into heat, which, when incorporated into liquid crystal polymers or other shape-changing polymers, induces localized heating and mechanical deformation. Other reported materials, such as azobenzenes and spiropyrans, embedded in similar polymer matrices, act as structural switches through trans–cis isomerization, generating internal stress gradients that produce visible deformations (*Figure 5B*).[164,168,169] Once the light stimulus is removed, the material reverts to its original configuration, enabling repeatable and reversible actuation.[164]

Shape-changing textiles offer precise light-driven actuation, with potential applications ranging from soft robotics (e.g., light-controlled grippers) to adaptive home textiles, including self-regulating, sun-responsive curtains.[170] They also present interesting opportunities in interactive art-textile installations, where sunlight can dynamically alter the structure of the fabric.[171] However, research on these materials remains limited, with insufficient experimental data for detailed analysis. As a result, shape-changing textiles were addressed only briefly in **Publication III**.

2.4.3 Self-healing textiles

Light-triggered self-healing in textiles enables the repair of mechanical damage via light exposure and can be implemented at the yarn level or in fabric coatings and surface finishes. Healing is commonly achieved by embedding healing agents within microcapsule or microvascular systems, although these can only repair damage a finite number of times.[172] More durable solutions use intrinsically renewable mechanisms, such as thermally reversible Diels–Alder reactions or dynamic disulfide bond exchange.[35] For example, polyurethane-based polymers containing dynamic disulfide bonds have shown healing efficiencies above 95 % at moderate temperatures (25–80 °C).[55,173] Incorporating light-responsive agents to these systems enables localized and efficient activation of self-healing process. Common examples include GO,[174,175] PDA,[176] and azobenzene derivatives.[30] Photothermal materials such as GO and PDA convert absorbed light into heat, raising the polymer matrix temperature to initiate healing,[55,175] while photoisomerization systems lower T_g to enhance chain mobility. For instance, Chen *et al.*[30] developed photohealable fabrics from polystyrene and azobenzene-containing polymer (PAzo), where UV light converted PAzo into a cis-isomer ($T_g \approx 13.7$ °C) to enable repair, and green

light reverted it to a rigid trans-isomer ($T_g \approx 53.5$ °C) to complete the cycle (*Figure 5C*).

Fabrics with this capability can repair minor mechanical damage after use, maintaining their performance over extended periods and reducing the need for replacement (see *Figure 1*). On a broader scale, self-healing textiles have the potential to reduce textile waste and support circular economy principles within the industry.[30,31] However, research in this field remains at an early stage, with only a few documented prototypes. Consequently, photoresponsive self-healing textiles were also addressed only briefly in **Publication III.**

2.5 Motivations to analyse photoresponsive textiles

According to Ilén *et al.*,[12] the development of photoresponsive smart textiles should prioritise their ability to deliver meaningful environmental and social values. Indeed, extensive research has highlighted their potential in applications such as energy conservation,[26,43,177,178] healthcare,[99,163,179,180] and thermoregulation[157,181–183] (see *Figure 1* and Sections *2.2–2.4*), often presenting them as sustainable alternatives to conventional solutions.

Achieving these benefits, however, requires that product design and development follow sustainability principles, ensuring that functionality, application-specific requirements, and life-cycle impacts are carefully aligned—from raw material selection and manufacturing to use and end-of-life processing.[12] Each additional material or processing step inevitably increases the environmental burden. Therefore, the added functionality must provide clear, measurable advantages that outweigh its environmental and resource costs.

Despite the suggested potential of photoresponsive textiles, major uncertainties remain regarding their practical performance, energy efficiency, and long-term environmental impacts. These uncertainties highlight the gap between the theoretical advantages often emphasized in the literature and their realistic use, raising important questions*: Can photoresponsive textiles reliably deliver promised functions and benefits? Are current testing protocols sufficient to translate laboratory results into real applications? What are their potential environmental costs, and can these be justified by claimed advantages?* For instance, photocatalytic textiles, often loaded with NPs, are promoted as resource-saving materials that reduce laundering frequency and thereby lower water and energy consumption.[43,177,178] Yet repeated washing can cause nanoparticle leaching, which not only reduces functional durability but may also pose environmental and health risks,[113] and these aspects are often missing from the literature. Perhaps more importantly, photocatalytic processes typically require prolonged light exposure (even up to several days) and light intensities that are rarely achievable even under

normal outdoor conditions let alone in indoor conditions. Consequently, self-cleaning appears unlikely in practice for many of the suggested applications making the claims of environmental benefits from reduced laundering to be overly optimistic.

Given the substantial environmental impact of the textile industry, developing photothermal textiles is only justified if their claimed benefits are demonstrated under realistic use conditions. Without such verification, the additional material requirements, production complexity, and end-of-life challenges involved in their manufacture, maintenance, and recycling are difficult to defend.[12] Addressing these considerations would be an important step toward transitioning smart textiles from laboratory prototypes to commercially viable products.

3 Experimental Section

Full details of the materials and methods used in the thesis can be found in the original publications (**I-III**). A summary of the key materials, fabrication and characterisation methods is given here. This chapter covers experimental information on photochromic (**Publication I**) and photocatalytic (**Publication II**) textiles (Sections *3.1–3.2*), as well as the methodology of literature search on critical analysis of photoresponsive smart textiles (Section *3.3;* **Publication III**)

3.1 Synthesis of photoresponsive smart textiles

3.1.1 Fabrics and their pre-treatment

Fabrics used in the study (white synthetic fabric (**I**) and undyed cotton fabric (**II**)) were cut into rectangular specimens and cleaned to remove residual impurities and enhance fiber surface activity for particle adhesion. Detailed info on fabrics and washing protocols can be found in their respective **Publications (I, II)**.

3.1.2 Photochromic minerals and their synthesis

The photochromic component of this study was synthetic hackmanite ($Na_8Al_6Si_6O_{24}(Cl,S)_2$), a mineral exhibiting reversible color transition from white to pink/purple under UV irradiation (UV-A/B/C) with reversion triggered by green light (λ = 530 nm; see details in *Figure 3C*).[70,85,87] This material was synthesized by Prof. Mika Lastusaari's group (University of Turku, Finland) following established protocols.[184]

The synthesis recipe of hackmanite-loaded coatings was modified from earlier procedures.[86,185] In our method, Benzyl Butyl Phthalate (BBP) was replaced by Di(isononyl)cyclohexane-1,2-dicarboxylate (DINCH) and Triton X-100 with Tergitol 15-S-9 to maintain comparable flexibility and adhesion while substantially enhancing biocompatibility.[186,187] Complete reagent specifications, including purities and suppliers, are detailed in **Publication I**.

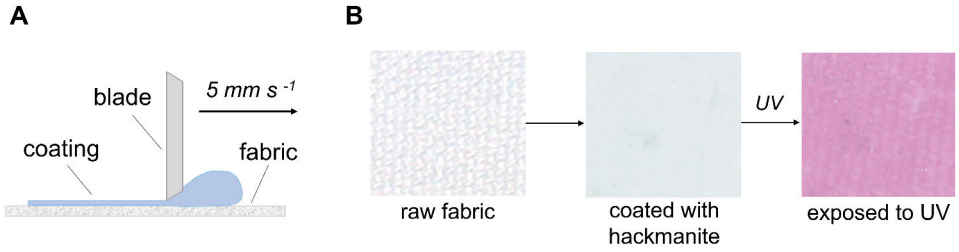

Figure 6. **(A)** Schematic illustration of the doctor-blading process. **(B)** Photographs of raw synthetic fabric (*left*), fabric coated with a hackmanite-loaded film before (*middle*) and after (*right*) UV-B-triggered coloration. **Publication I**; Adapted under terms of the CC-BY license.[22] Copyright 2024, The Authors, published by Elsevier B.V.

The coating paste was prepared by planetary milling hackmanite powder (0.68 g) with ethanol, 2-butanone, and Tergitol 15-S-9 for 10 min, followed by the addition of PVB binder and DINCH plasticizer, and an additional 2 min of milling. The resulting mixture was applied to synthetic fabric using the doctor blade method at 5 mm s^{-1} (*Figure 6A*), a technique selected for its operational simplicity, precise thickness control, and scalability.[41] The as-prepared samples were then dried under controlled conditions (10 min, < 30 % RH), yielding a film with approximately 73 % hackmanite loading (*Figure 6B*). Further analysis of these samples is presented in Sections *4.1–4.3, 4.5* and *4.6*.

3.1.3 Fabrication of photocatalytic NPs and their application onto textiles

In **Publication II**, flower-like ZnO NPs for self-cleaning textiles were synthesized via a combination of sol–gel and microwave-assisted methods, adapted from other protocols.[65,188,189] Synthesis parameters such as microwave irradiation time (3–5 min), zinc precursor concentration (0.05–0.3 M Zinc Acetate Dihydrate (ZnAc)), solvent type (deionized water (DI H_2O) or ethanol), and precipitating agent concentration (0.1–0.3 M NaOH or 1–2 ml NH_4OH) were systematically varied and optimized. Since the literature indicates that flower-like crystals (see *Figure 10* in Section *4.2*) achieve the best self-cleaning performance,[130] this study specifically focused on identifying synthesis conditions that produce such morphologies. NH_4OH adjusted pH and stabilized the reaction medium, removing the need for harmful surfactants like cetrimonium bromide, commonly used for morphology control but omitted here in line with green chemistry principles.[126]

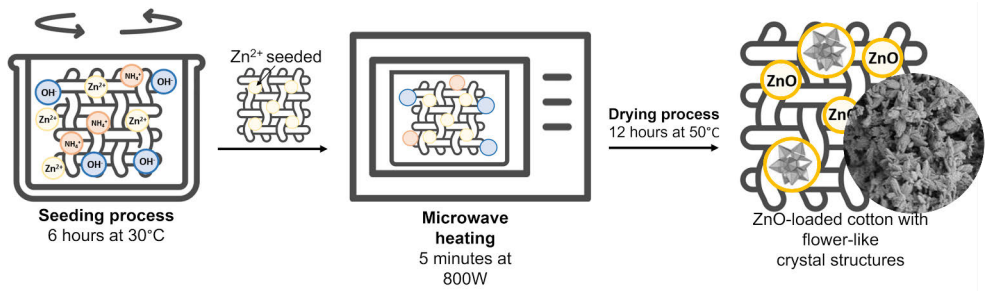

Figure 7. Schematic illustration of a representative process for fabricating flower-like ZnO crystal structures on a cotton substrate: seeding process (*left*), microwave-assisted synthesis (*middle*), and the resulting ZnO-coated cotton sample with an SEM image of the flower-like structures and its graphical representation (*right*). **Publication II**; Adapted under terms of the CC-BY license.[24] Copyright 2023, The Authors, published by Elsevier B.V.

In a representative synthesis yielding the most desired flower-like crystal structures, ZnAc (0.2 M) was dissolved in ethanol and mixed with 0.1 M NaOH (33:66 ml) under vigorous stirring, followed by the addition of 2 ml NH_4OH to produce a hazy suspension (pH ~ 11). Cotton substrates were immersed in this solution for 6 h to promote crystal nucleation prior to microwave treatment (800 W, 5 min). The samples were then rinsed with deionized water to remove unattached particles and dried in an oven at 50 °C for 12 h (see *Figure 7*). Examples of the parameters modified in this protocol and analyzed in this thesis are summarized in Table *2*, with further discussion in Sections *4.1, 4.2, 4.4*, and *4.5*. Table *2* presents the conditions whose variation led to significant differences in the resulting crystal morphologies. Full reagent specifications, including purities, suppliers, and the complete list of tested parameters, are provided in **Publication II** and its Supporting Information.

Table 2. Examples of various parameters and conditions used for synthesis of ZnO NPs on cotton analysed in this thesis, relevant for further discussion provided in Sections *4.1*, *4.2*, *4.4*, and *4.5*. **Publication II**; Adapted under terms of the CC-BY license.[24] Copyright 2023, The Authors, published by Elsevier B.V.

Sample ID	Zn Precursor Concentration (mM)	Solvent Type	Precipitating Agent Concentration	MV time (min)
0.1NaOH_30°C	20	DI H_2O	0.1 M NaOH	4
0.1NaOH_t3	20	DI H_2O	0.1 M NaOH	3
0.1NaOH_t5	20	DI H_2O	0.1 M NaOH	5
DIEtOH_Z	20	DI H_2O + ethanol	0.1 M NaOH	5
EtOH_Z	20	ethanol	0.1 M NaOH	5

3.2 Characterization methods

3.2.1 Crystalline structures analysis (XRD)

X-ray powder diffraction (XRD) was employed to identify crystal structures in both **Publications I** and **II**, using a PANalytical Aeris diffractometer (40.0 kV, 7.5 mA for Publication I and 45.0 kV, 40.0 mA for Publication II) with CuKα1 radiation. Detailed operating parameters are available in the corresponding **Publications (I, II**).

3.2.2 Surface morphology analysis (SEM)

Surface morphologies of both coatings (**I, II**) were analyzed using a Thermo Scientific Apreo S field emission scanning electron microscope (FE-SEM). Photochromic textile samples (**I**) were examined under low vacuum conditions (H_2O, 100 Pa chamber pressure, 2.0 kV acceleration voltage and 100 pA currents), while ZnO-coated samples (**II**) were analyzed at 2.0 kV and 25.0 pA currents. Detailed operating parameters are available in the corresponding **Publications (I, II)**.

3.2.3 Color coordinates, reflectance and light responsive measurements

The photochromic (i.e., color-changing) properties of the hackmanite-coated fabrics (**Publication I**) were evaluated through color coordinate analysis (Lab* color space) and reflectance spectroscopy. Color coordinates were measured using a Konica Minolta CM-2300d spectrophotometer (D65 illuminant, 10° observer). Reflectance spectra were recorded with an Avantes AvaSpec HS-TEC spectrometer coupled to a 1000 μm Vis/NIR fiber optic probe, using MgO as a white reference and the black current as a baseline. Note that the low light intensity below approximately 550 nm in this setup can result in an increased noise level in the measured spectra (see Figure *11B* in Section *4.3*). Prior to measurements, samples were UV-B irradiated (Analytikjena UVM.57 Handheld UV Lamp, 6 W, 302 nm) at 3 J cm^{-2} to achieve maximum photochromic coloration.

Since higher UV flux is directly linked to an increased stochastic risk of epidermal damage and skin carcinogenesis, quantifying the photoresponse time is particularly relevant for UVI-monitoring applications. Rapid response performance was measured under UV irradiation at 302 nm and 365 nm (Analytikjena UVLS-24 EL Series UV Lamp, 4 W, 365 nm) at various irradiance levels (5–25 W m^{-2}) for 10 min. Dedicated Avantes spectrometers (ULS2048CL-EVO for 302 nm, HS-TEC for

365 nm) were employed. Reflectance measurements used optimized illumination sources (40 W incandescent for 302 nm, Ocean Optics LS-1 for 365 nm) to minimize specular reflection. Data were collected at intervals as detailed in Figure *11(C–D)* in Section *4.3*. Further details on reflectance measurements are provided in **Publication I**.

3.2.4 Evaluation of fading rate and color fatigue resistance

Assessment of color reversibility is as important as coloration testing, since it determines the practical reusability of UV-sensing tools; rapid color reversion to the baseline state enables consecutive measurements without operational delays. To evaluate the fading rate, hackmanite-coated fabrics were UV-B irradiated for 10 min to reach maximum coloration, then placed under a solar simulator (AM1.5 spectrum, LOT Quantum Design LS0500 with Edinburgh Instruments 495 nm long-pass filter) for 70 min until complete bleaching. Reflectance spectra were recorded using the setup described above (Section *3.2.3*), with data collected at predetermined intervals as specified in Section *4.3*.

Color fatigue resistance was assessed to determine the durability of the color-changing functionality by tracking color saturation over repeated photochromic cycles. Measurements followed the same experimental setup used for color coordinate analysis (Section *3.2.3*). The coloration cycles were evaluated by comparing the color coordinate values of both maximum coloration and fully bleached states over 20 cycles.

3.2.5 UV-VIS analysis and UPF values

ZnO-coated samples (**Publication II**) were analyzed using UV–Vis spectrophotometry (200–700 nm) to assess their UV-blocking performance before and after 48 h of extensive sunlight exposure (see Section *3.2.6* for details). Measurements were performed on both untreated and ZnO-treated fabrics. UV-A (315–400 nm) and UV-B (280–315 nm) blocking percentages were calculated using standard equations (*Eq. 1* and *Eq. 2-3* in Publication II). Values of E(λ) and S(λ) were taken from AS/NZS 4399:1996,[147] T(λ) values were obtained from UV–Vis measurements, and Δλ was set to 5. More details on UV-Vis measurements are available in **Publication II**.

3.2.6 Performance evaluation based on photoanalysis

Photoanalysis was employed for two purposes: (1) evaluating the relationship between color saturation and UVI values in photochromic fabrics (**Publication I**)

and (2) conducting self-cleaning tests with subsequent stability assessment of ZnO-coated samples under prolonged sunlight exposure (**Publication II**). For UVI-dependent color change measurements of hackmanite-coated fabrics, samples were irradiated simultaneously with 302 nm (UV-B) and 365 nm (UV-A) light for 10 min at controlled UVI levels of 1, 3, 5, and 7, representing Earth-surface relevant conditions.[70] UVI was monitored using a Solarmeter® Model 6.5, and color changes were documented under standard room lighting. The G:G ratio (white-to-colored state) from RGB (red, green, blue) analysis enabled calibration of the Sensoglow app for UVI determination based on material-specific color response.[190] Additional details are available in **Publication I**.

The self-cleaning performance of ZnO-coated cotton fabrics was evaluated through controlled staining tests under simulated sunlight. Test samples, including ZnO-treated and untreated reference fabrics, were stained with 10 µL of drip coffee and 10 µL of MB solution (0.005 g/ 100 mL DI H_2O). Stained fabrics were exposed to artificial sunlight using an Atlas XLS+ solar simulator equipped with an NXE 1700 xenon lamp (AM1.5G spectrum) for 48 h, corresponding to a total UV dose of ~ 11,000 kJ m^{-2} (300–400 nm) at ~ 36 °C and ~ 10 % RH. This total UV dose is equivalent to approximately 15-17 days of outdoor exposure in central Europe.[191] To monitor stain degradation, samples were periodically removed from the simulator for imaging under controlled lighting conditions, following the protocol in **Publication II**. Images were processed in Adobe Lightroom Classic for white balance and color profile correction. Self-cleaning efficiency was quantified through Python-based analysis of average RGB values from three predefined regions per stain type. Untreated control samples were used to distinguish photocatalytic effects from potential substrate aging under prolonged UV exposure. Color analysis of these samples was further applied to evaluate long-term color stability (i.e., aging).

3.2.7 Durability testing

Durability tests were conducted to evaluate how well the photochromic coating adhered to the textile surface under mechanical stress (**Publication I**). The flexibility of hackmanite-coated samples was assessed using a Satra Upper Material Flexing Machine (STM 407) for 500 cycles. Post-flexing samples were examined under an optical microscope (Tagarno Trend) for coating cracks. Moreover, to visually assess sample flexing, sun-shaped color patterns were created using UV-B light (302 nm) and a hand-made photomask (see *Figure 6A* in Publication I), and captured with a Canon EOS 250D camera.

Washing durability was evaluated using a standardized washing method (EN International Organization for Standardization (ISO) 6330:2021). Photochromic fabrics were first UV-colored (302 nm, Analytikjena UVP UVLMS-38) and then

subjected to five washing cycles (30 °C, 30 min). Samples were subsequently oven-dried (50 °C, 4 h) following a standardized method for microplastic mass loss (ISO 4484-1:2023). Post-washing analysis included gravimetric assessment (Kern&Sohn ABT 220-5DNM) for coating mass loss, microscopic examination (Tagarno Trend) for physical changes, and spectrophotometric evaluation (Konica Minolta) for color fastness.

3.3 Methodology for literature search

To identify and analyze key research motivations in non-electronic photoresponsive textiles for **Publication III**, a systematic literature review was conducted. The analysis examined peer-reviewed journal articles from 2020–2022 using keyword-based queries in the Web of Science database, focusing on five textile functions: self-cleaning (photocatalytic), photochromic, photothermal, shape changing, and self-healing. Search outcome was limited to light-activated textiles without embedded electrical circuits, excluding, for example, photovoltaic textiles. Moreover, the analysis followed standardized technical textile classifications,[192] focusing specifically on wearable and household applications while excluding non-textile substrates like water treatment membranes.

Thus, a four-step screening process was implemented: (1) keyword selection targeting light-driven functionalities within the specified timeframe (a complete keyword list in *Table 1* in Publication III), (2) exclusion of review and perspective articles, (3) filtering out publications from journals with impact factors ≤ 1 and conference papers, and (4) manual evaluation of abstracts and introductions to verify alignment with research scope. The complete listing of publications included in this study and those manually excluded are provided in Supporting Information in **Publication III**.

4 Results and Discussion

The *results and discussion* section is organised into two parts. The first part (Sections *4.1–4.6*) presents the results on textiles coated with photochromic (**Publication I**) and photocatalytic materials (**Publication II**), focusing on UV monitoring (**I**) and self-cleaning with UV-blocking (**II**) functionalities. These sections discuss the experimental findings, highlighting the properties and photoresponsive behavior of the developed textiles. The second part (Section *4.7*) offers a critical assessment of non-electronic photoresponsive textiles, evaluating whether they meet their sustainability claims and functional promises under intended working conditions (**Publication III**). This analysis, based on 130 peer-reviewed studies, identifies key performance challenges and outlines directions for future research.

4.1 Crystalline structures analysis (Publications I, II)

To verify that the chemical composition of the hackmanite powder used in **Publication I** matched the expected one, XRD analysis was performed. The measured pattern was indeed consistent with entry 04-017-7136 ($Na_8Al_6Si_6O_{24}S_{0.1}Cl_{1.8}$) in the Powder Diffraction File™ (PDF)-4+2021 database, with no additional phases detected (*Figure S1* in Publication I), confirming the expected composition.

In **Publication II**, XRD analysis of coated cotton samples was performed to confirm ZnO deposition on the fabric surface and to check for possible traces of $Zn(OH)_2$. The latter can form due to incomplete dehydration of $Zn(OH)_2$ to ZnO during synthesis and, unlike ZnO, exhibits no photocatalytic activity.[193] XRD results confirmed successful ZnO formation in most samples (*Figure 8*), with characteristic cellulose reflections from the cotton substrate appearing at 14.8°, 16.5°, and 22.7°.[194] The ZnO peaks observed at 31.74° (100), 34.38° (002), 36.22° (101), 47.54° (102), 56.58° (110), and 62.82° (103) correspond to the hexagonal wurtzite structure (PDF entry 00-036-1451),[195,196] indicating phase-pure crystalline growth on the cotton substrate.

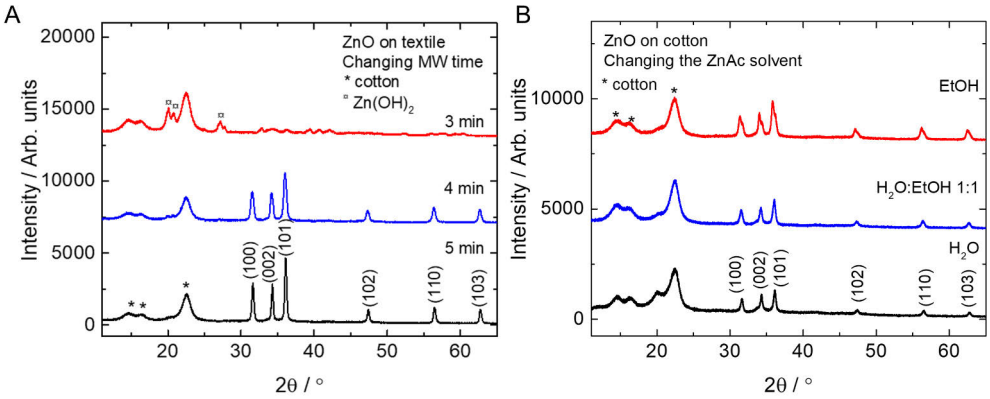

Figure 8. XRD patterns of ZnO and $Zn(OH)_2$ crystals formed on cotton substrates using a representative synthesis procedure modified by **(A)** changing microwave times, and **(B)** changing solvent for ZnAc solution. **Publication II**; Adapted under terms of the CC-BY license.[24] Copyright 2023, The Authors, published by Elsevier B.V.

XRD analysis revealed several factors that influence the conversion of $Zn(OH)_2$ to ZnO, with microwave irradiation time (*Figure 8A*) and precipitating agent concentration (0.1–0.3 M NaOH) being particularly significant (see *Figure 3A* in Publication II). Microwave treatment duration showed a clear correlation with ZnO peak intensity, indicating the extent of phase conversion. A 3-min treatment left residual $Zn(OH)_2$, suggesting insufficient energy for complete dehydration, whereas extending the treatment to 4–5 min markedly enhanced ZnO formation, as evidenced by the stronger XRD signals (see blue and black patterns in *Figure 8A*).

The solvent composition used for ZnAc solution preparation was also varied, from pure H_2O (reference sample 0.1NaOH_t5) to a 1:1 H_2O:EtOH mixture (sample DIEtOH_Z) and pure EtOH (sample EtOH_Z), to assess its effect on ZnO growth (*Figure 8B*).[197] However, all three solvents produced similar ZnO peak intensities, indicating no substantial solvent-dependent differences. Note that while post-synthesis annealing up to 600 °C can convert $Zn(OH)_2$ to phase-pure ZnO for powder or temperature-resistant substrates,[131,198] this step was omitted due to the gentle nature of fabrics. Consequently, samples containing $Zn(OH)_2$ patterns were excluded from further analysis.

4.2 Surface morphology analysis (Publications I, II)

In **Publication I**, SEM analysis was used to examine the uniformity of hackmanite distribution within the fabricated coating and its penetration into synthetic fabric (*Figure 9*). The coating morphology showed hackmanite crystals embedded in a thin plasticizer layer, with moderately uniform distribution despite some structural irregularities and agglomeration (*Figure 9A–B*). Cross-sectional imaging further

revealed substantial solution penetration beyond the surface layer. Since the substrate was synthetic with a highly hydrophobic surface, such pronounced infiltration is noteworthy. This result can be attributed to the reduced surface tension of ethanol, used in the coating formulation, which promoted penetration into the hydrophobic matrix (*Figure 9C*).

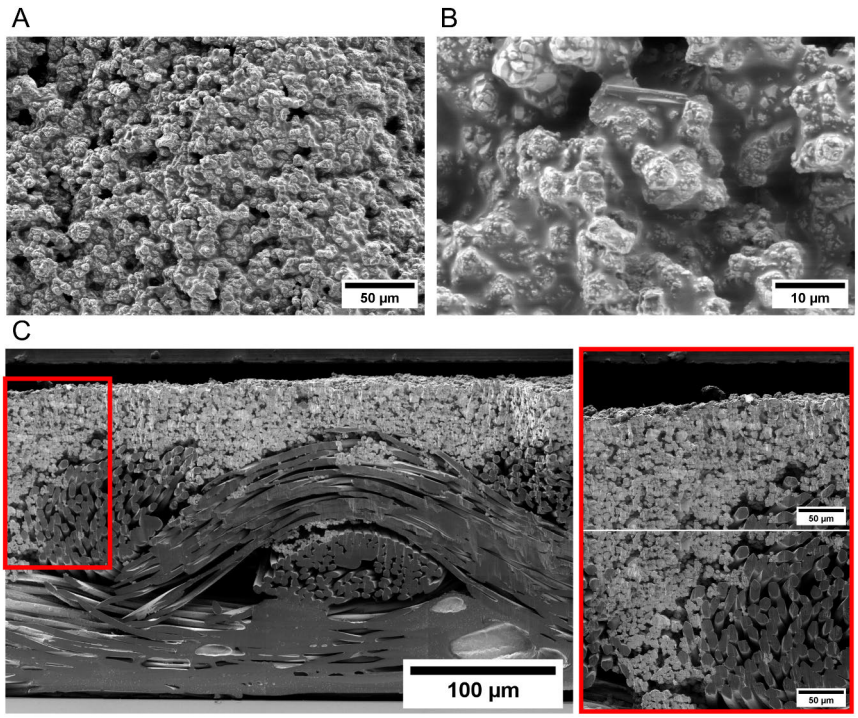

Figure 9. SEM images of hackmanite-coated fabric, showing **(A)** top-down view of the sample surface, **(B)** magnified top-down view of hackmanite crystals and their morphology, and **(C)** cross-sectional view highlighting the fabric-coating interface, with magnified details on the right. **Publication I**; Adapted under terms of the CC-BY license.[22] Copyright 2024, The Authors, published by Elsevier B.V.

In **Publication II**, SEM imaging was used to examine the morphology of ZnO crystals grown directly on cotton substrates, providing complementary insights to the XRD analysis. While ZnO patterns were detected in most samples, the primary objective of this study was to obtain flower-like ZnO structures. SEM analysis was therefore essential for identifying and characterizing these morphologies, including particle distribution and crystal shape. SEM images of representative samples are available in Figure *10*.

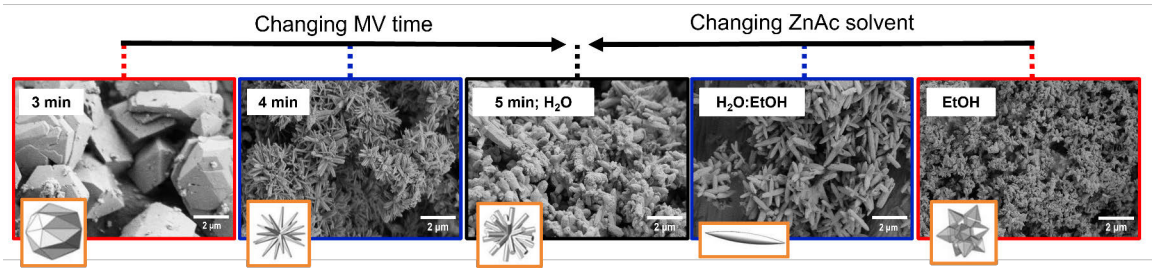

Figure 10. SEM images of ZnO and $Zn(OH)_2$ crystal structures on cotton substrates prepared using a representative synthesis, with variations in microwave irradiation time (*left three images*) and solvent composition for ZnAc (*right three images*), along with a graphical representation of the resulting crystal morphologies (*orange framed*). The middle image (5 min; H_2O) is common to both sets. Frame colors of SEM images correspond to XRD results shown in Figure *8*. Obtained morphologies are named according to[131] as follows (*from left to right*): narcis-like, flower-like, flower-like, needle-like and flower-like structures. SEM images adapted under terms of the CC-BY license (**Publication II**).[24] Copyright 2023, The Authors, published by Elsevier B.V. Graphics adapted by permission of Informa UK Limited, trading as Taylor & Francis Group, https://www.tandfonline.com.[131] Copyright 2018.

Reducing the NaOH concentration from 0.3 to 0.1 M induced a structural transition from flake-like to flower-like crystals (*Figure 3B* in Publication II). Detailed imaging indicated that the flower-like structures were composed of needle- and sword-shaped substructures, with diameters ranging from 500 nm to 1 µm. SEM observations also confirmed the link between synthesis time and $Zn(OH)_2$/ZnO crystal formation (*Figure 10*). For instance, the 3 min microwave sample (0.1NaOH_t3; *Figure 10*) contained bulky $Zn(OH)_2$ crystals along with ZnO nanoparticles. Longer irradiation altered the morphology, suggesting that smaller ZnO features formed via decomposition of larger $Zn(OH)_2$ particles. The 4 min sample (0.1NaOH_30°C) demonstrated marked particle aggregation, whereas the 5 min sample (0.1NaOH_t5) achieved broader particle distribution and more uniform surface coverage. Based on these observations, 5 min irradiation was selected as optimal and subjected to further modification.

Although solvent variation in ZnAc solutions (samples 0.1NaOH_t5, DIEtOH_Z, and EtOH_Z) did not significantly affect XRD patterns (*Figure 8B*), it noticeably influenced crystal shape. SEM imaging (*Figure 10*) revealed consistent needle- and sword-like morphologies across all solvents, but differences in particle sizes were evident. The EtOH_Z sample exhibited smaller, well-defined flower-like particles with a bulkier crystal shape compared to those obtained after 4 minutes of microwave irradiation, along with optimal surface coverage. Note that achieving uniform coverage and preventing aggregation is critical because the size of ZnO aggregates directly affects photocatalytic reactivity. Smaller aggregates promote higher hydroxyl radical formation, whereas larger aggregates reduce efficiency and

are difficult to break once formed.[199,200] Therefore, the most desirable morphology was an even distribution of ZnO flower-like crystals, as observed in samples 0.1NaOH_t5 and EtOH_Z. Such structures were expected to deliver strong self-cleaning performance (see Section *4.5 Performance evaluation based on photoanalysis* for results).

4.3 Photochromism and performance of hackmanite-coated fabric: color coordinates, reflectance, and light-responsive measurements (Publication I)

The photochromic response was evaluated to determine whether the hackmanite-coated textile changes color upon UV exposure. As expected, the coating exhibited a pronounced transformation under UV-B irradiation, confirming the successful fabrication of a UV-responsive textile. The samples rapidly shifted from off-white to deep purple, a transition detectable both visually (*Figure 6B*) and through quantitative measurements (*Figure 11A–D*). The chromaticity diagram in the International Commission on Illumination (CIE)-1931 color space (*Figure 11A*) shows three distinct points: the uncoated white fabric substrate, the coated fabric, and the UV-B-saturated coated fabric. Reflectance spectra provided a more detailed view of the photochromic behavior *(Figure 11B*). Without UV irradiation (see blue line in *Figure 11B*), the spectrum of the hackmanite-coated sample displays only a slight, uniform decrease across the visible range (400–700 nm). An absorption band at ~ 580 nm originates from the partial transparency of the hackmanite layer, which allowed the yellow absorption band of the underlying fabric to remain partly visible. Upon UV exposure (see purple line in *Figure 11B*), the sample color changed, defined by a broad absorption band in the green region (~ 540 nm) of the spectrum, which appears as a purple hue to the naked eye.[70] The minor signal fluctuations observed in Figure *11B* below 550 nm are due to reduced lamp intensity in this range and are characteristic of this measurement setup.

Monitoring response time is another key aspect of testing photochromic materials, as it reflects their suitability for UV sensing applications; users are unlikely to wait hours to determine UVI values. Since UV-A and UV-B wavelengths largely determine the UVI, these spectral regions were selected to evaluate the time-dependent color response over a 10-minute period. As shown in Figure *11(C–D)*, both UV-A and UV-B exposure induced measurable color changes within just 15 s. The response dynamics followed expected photon-interaction statistics: lower intensities (5–15 W m^{-2}) produced slower coloration rates due to reduced color-center formation probability, while higher intensities (25 W m^{-2}) accelerated the response. Notably, slight solarization was observed at 25 W m^{-2} after 7 s, indicating

partial loss of coloration once a sufficiently high dose was reached.[67] As color saturation was achieved after 10 min, this duration was used as the standard exposure time for subsequent measurements in Section *4.3.1*.

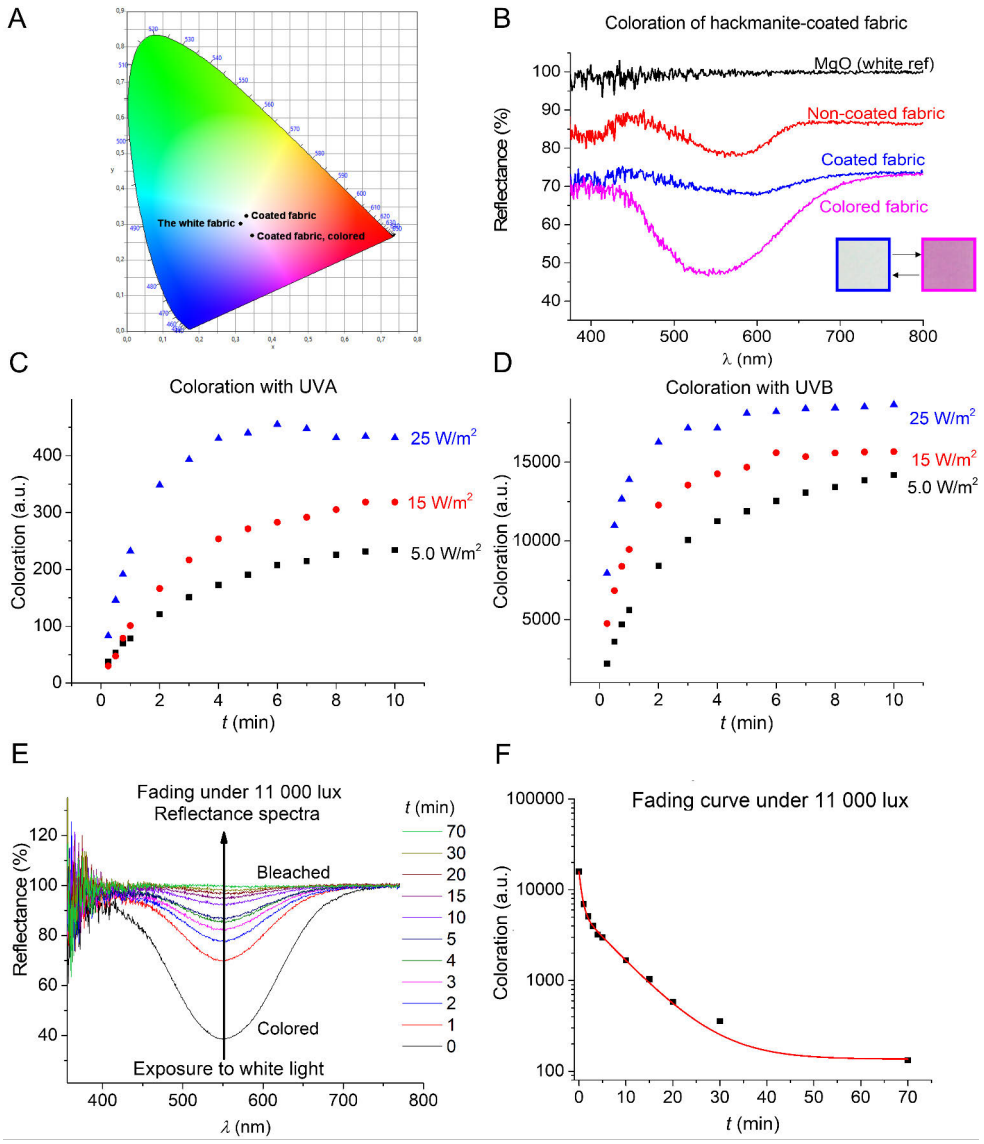

Figure 11. **(A)** CIE-1931 color space distribution of hackmanite-coated fabric determined from color coordinate measurements. **(B)** Sample reflectance spectra before and after UV-B irradiation. **(C)** Time-dependent coloration kinetics under UV-A and **(D)** UV-B exposure at irradiances of 25, 15, and 5 W m^{-2}, respectively. **(E)** Reflectance spectra during fading of hackmanite-coated fabric exposed to white light (> 495 nm) and **(F)** coloration intensity versus fading time relationship. **Publication I**; Adapted under terms of the CC-BY license.[22] Copyright 2024, The Authors, published by Elsevier B.V.

4.3.1 Evaluation of fading rate and color fatigue resistance

Moreover, evaluating the fading rate is also necessary to determine the practical usability of UV-monitoring textiles, since only convenient fading times and conditions would support their repeated use. Interestingly, when the colored hackmanite-coated fabric was left in sunlight (e.g., on a windowsill), the purple coloration gradually faded until it disappeared completely (see *Figure S4* in Publication II). However, to accelerate and quantify this bleaching process, fully saturated samples were exposed to filtered solar irradiation (λ > 495 nm), which suppressed photochromic activation while promoting fading (see Section *4.5* for details). The resulting reflectance spectra showed a gradual increase in reflectance, approaching the 100 % value of the uncolored reference under visible light exposure (*Figure 11E–F*). As demonstrated in Figure *11E*, complete fading occurred within 50 min, as evidenced by spectral overlap with the original uncolored fabric. Figure *11F* further shows that the fading curve plateaued at 50 min and remained stable for the remainder of the 70 min measurement period, confirming the reversibility of the coloration. These data are used as the basis for evaluating color stability over repeated photochromic cycles.

As noted in Section *2.2.1*, reliable UV sensors should consistently reach the same level of color saturation after repeated use, ensuring users can trust their performance over multiple cycles. Previous studies showed that synthetic hackmanite retains its color fatigue resistance for at least 13 cycles without loss of saturation.[69] In the present work, fatigue resistance testing confirmed stable photochromic performance for a minimum of 20 cycles, with no measurable decline in color intensity (*Figure 13A*). Minor fluctuations in coating values were observed but are attributed to normal variation in spectral measurements. As discussed in **Publication I**, the exceptional color stability of hackmanite arises from its mineral composition. The coloration mechanism is driven by short-range electronic transitions within a robust crystal lattice, with tenebrescence protected by the mineral framework (see *Figure 3C*). While minor geometrical rearrangements occur at the color center and within the associated disulfide ion, these changes are subtle enough to proceed without breaking chemical bonds during repeated coloration and bleaching,[69] resulting in the reported color stability.

4.4 UV-VIS analysis and UPF values (Publication II)

The UV-blocking performance of the fabrics was assessed by UV–Vis spectroscopy and quantified through UPF values and ratings to evaluate how effectively the ZnO-coated textiles could protect the user from UV irradiation. Considering that extended sunlight exposure has been reported to enhance the self-cleaning effect, testing

whether these textiles provide solid UV protection is necessary to ensure safe use. The measurements were carried out on both untreated and coated samples, with UV-A (315–400 nm) and UV-B (280–315 nm) blocking percentages calculated using standard equations (*Eq. 1* and *Eq. 2–3* in Publication II) before (*Figure 12A, C*) and after (*Figure 12B, C*) extensive sunlight exposure (see Section *4.5*). To illustrate these effects, representative results for samples 0.1NaOH_t5, DIEtOH_Z, and EtOH_Z are discussed in detail below (*Figure 12*), while full spectral data for all investigated samples are provided in **Publication II**.

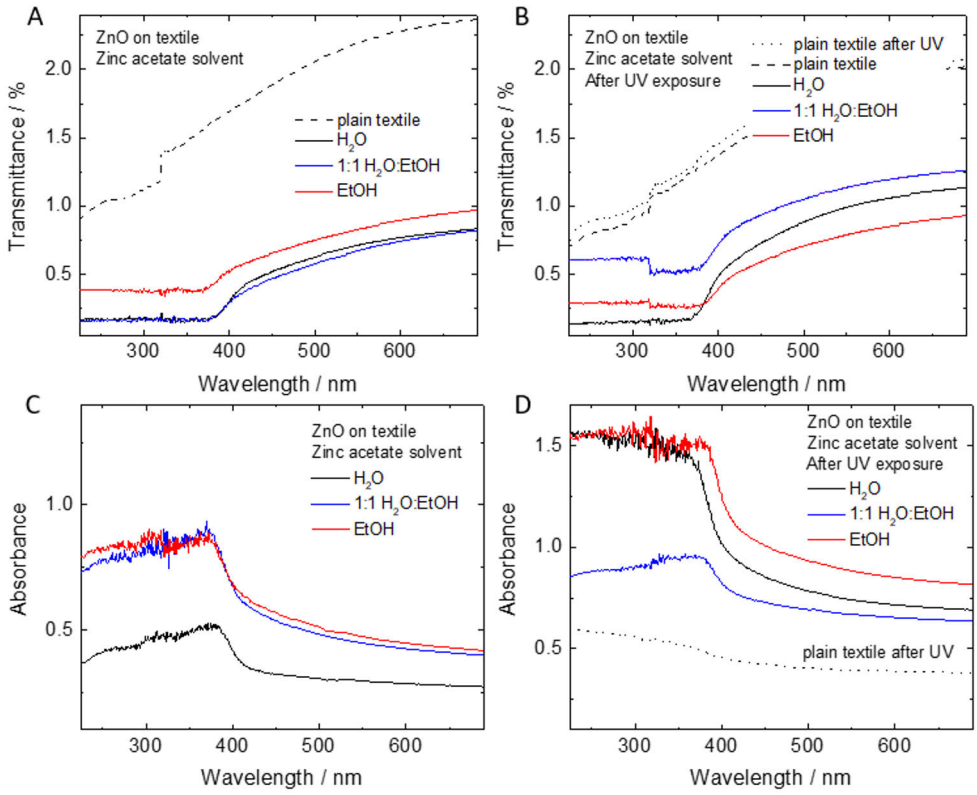

Figure 12. Transmittance and absorbance measurements of ZnO-coated cotton samples fabricated using different solvents for preparing ZnAc solution, before **(A, C)** and after **(B, D)** aging tests. **Publication II**; Adapted under terms of the CC-BY license.[24] Copyright 2023, The Authors, published by Elsevier B.V.

As mentioned in Section 2.3, ZnO particles effectively absorb UV radiation (< 360 nm) due to their wide bandgap ($E_{bg} \approx 3.3$ eV).[196,201] Thus, as expected, all ZnO-coated samples showed reduced transmission compared to the reference sample, particularly in the UV region. Samples containing flower-like structures (0.1NaOH_t5 and EtOH_Z) achieved nearly 100 % UV blocking and approximately 99 % visible light

blocking. Post-aging UV–Vis measurements, taken after 48 h of sunlight exposure, showed only minor transmission differences (~ 1 %) across all samples, which are likely attributable to natural sample variation or measurement error.

All samples achieved UPF values > 50 ("excellent protection"), consistent with previous studies [146]. Notably, some samples, such as 0.1NaOH_t5 and EtOH_Z, exceeded UPF 800, demonstrating extremely high UV protection (*Table 3*). Sample EtOH_Z showed exceptional performance (UPF = 1040; UV-A = 99.9 %; UV-B = 99.9 %), likely due to its high surface coverage and favorable flower-like crystal morphology. These UV-A and UV-B blocking efficiencies are consistent with literature[65] and surpass ZnO coatings using arginine surfactants (UV-A ~ 80 %, UV-B 60–90 %)[196]. Interestingly, even plain cotton exhibited high UV protection (UPF = 81, UV-A = 98.5 %, UV-B = 98.8 %), most likely due to its dense fiber structure. This finding suggests that ZnO deposition on lower-UPF textiles, such as viscose (UPF = 3.0),[202] could provide an even greater relative improvement in protection.

Table 3. UPF and the UV-A and UV-B blocking efficiency and UPF classification of ZnO-coated samples synthesized using different solvents for preparing ZnAc solution. **Publication II**; Adapted under terms of the CC-BY license.[24] Copyright 2023, The Authors, published by Elsevier B.V.

Sample ID	UPF value	UV-blocking efficiency (%)		UPF classification
		UV-A	UV-B	
Reference sample	81	98.49	98.83	excellent protection
0.1NaOH_t5	883	99.89	99.93	excellent protection
DIEtOH_Z	191	99.59	99.64	excellent protection
EtOH_Z	1040	99.91	99.94	excellent protection

4.5 Performance evaluation based on photoanalysis (Publications I, II)

In **Publication I**, photoanalysis was used to investigate how color saturation in the hackmanite-coated sample correlated with the UVI values it was exposed to. As discussed in Section *2.2.1*, numerous studies have suggested that hackmanite could serve as an effective active material for UV sensing applications.[21,70,87] When exposed to UV light, it undergoes visible color changes that can be interpreted even by untrained users[70] (see an example in *Figure 6B*). Figure *13B* shows that the hackmanite-coated fabric indeed exhibits detectable coloration already at UVI levels below 3—the established threshold for sunburn prevention measures.[70,97] The upper UVI limit for testing was set at 7, as this value precedes the point where radical preventive actions become necessary, however, the material is expected to remain functional at higher UVI values.

Visual inspection alone may not provide precise UVI values, so color saturation should be complemented with more accurate measurements for real-world use. Since average users are unlikely to assess the color changes of hackmanite-coated fabrics using conventional reflectance measurements, **Publication I** introduced a more practical solution, the proprietary Sensoglow mobile app (*Figure 13C*). The app determined the exact UVI by photographing UV-exposed samples and comparing their coloration to calibrated reference states (uncolored and fully colored) associated with specific UVI values. In this way, users can obtain reliable readings without concern for variations in lighting conditions during image capture. Since ambient visible light gradually bleaches hackmanite, practical use of this sensor would require short-pass filters to support accuracy, as described in **Publications I** and **III**.

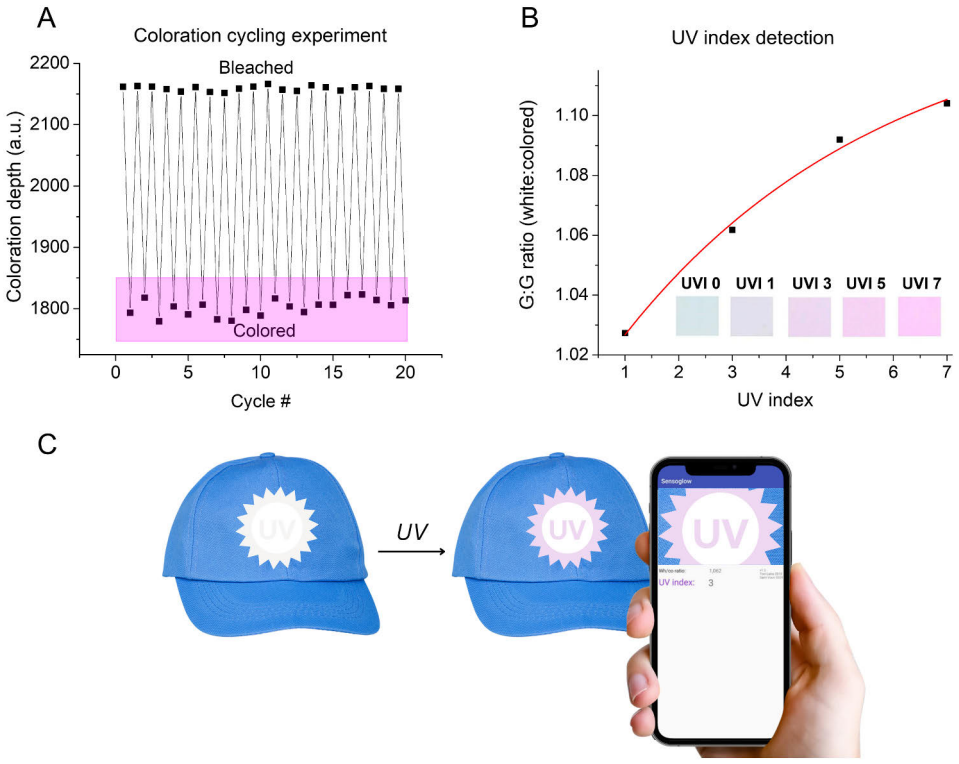

Figure 13. **(A)** Photocycles of hackmanite-coated fabric, alternately exposed to UV-B and visible light. **(B)** Color intensity variations of this fabric, corresponding to different UVI levels. **(C)** Schematic demonstration of a hackmanite-based UV sensor, printed on a cap. This example illustrates how it can indicate UV exposure levels through color intensity changes, which can be monitored visually or through the proprietary Sensoglow app. **Publication I**; Adapted under terms of the CC-BY license.[22] Copyright 2024, The Authors, published by Elsevier B.V.

In **Publication II**, photoanalysis was used to assess both the self-cleaning efficiency and long-term stability of ZnO-coated textiles under prolonged sunlight exposure. All samples containing ZnO were stained and then subjected to artificial sunlight in a solar simulator for 48 h. The samples analyzed here included uncoated cotton (reference) and three ZnO-coated variants (0.1NaOH_30°C, 0.1NaOH_t5, and EtOH_Z), chosen for their flower-like morphologies and optimal coverage. The results for other samples are reported in **Publication II**.

As demonstrated in Table *4*, RGB values of the coating background, MB stains, and coffee stains were analyzed separately. Color deviation was quantified by calculating Euclidean distances of RGB values at different time points to determine percentage variation.[203] Differences in surface energy among coatings led to varied droplet–fabric interactions and, consequently, different initial stain intensities (see stain shapes in *Table 4*).

All samples exhibited noticeable fading of MB and coffee stains after 5 h of solar exposure, though at different rates. The reference sample showed 33 % MB discoloration after 1 h and 70 % after 24 h. Samples 0.1NaOH_30°C and 0.1NaOH_t5 achieved slightly higher values, with 40 % and 51 % discoloration after 1 h, increasing to 74 % and 77 % after 24 h, respectively. In contrast, EtOH_Z demonstrated markedly better performance, reaching 73 % discoloration after 1 h and 90 % after 24 h. Note that 1 h of solar exposure under an artificial sun corresponds to approximately 8 h of real-world sunlight exposure, indicating that one sunny day could be sufficient to obtain a significant change (see Section *3.2.6* for details).

Coffee stain removal followed a similar trend. The reference fabric achieved only 15 % removal after 1 h, while 0.1NaOH_30°C and 0.1NaOH_t5 reached 22 % and 53 % after 1 h, increasing to 64 % and 60 % after 24 h, respectively. Again, EtOH_Z performed best, with 32 % removal after 1 h and 82 % after 24 h. These findings indicate that optimal photocatalytic performance depends not only on crystal morphology but also on surface coverage and particle size, all of which must be equally considered to produce effective self-cleaning textiles. Notably, these results were obtained at RH of approximately 10 %, which is particularly interesting given that previous studies reported no coffee stain degradation under low-humidity conditions, requiring ≥ 60 % RH for measurable activity.[65]

The same photoanalysis method was applied to evaluate coating stability and potential substrate degradation after 48 h of intense sunlight exposure (see *Table S5* in Publication II). Accelerated aging tests with artificial sunlight are a standard technique to predict the long-term performance of light-activated materials, particularly in applications like this one, where effective stain removal may require extended exposure. As expected, all samples displayed a gradual lightening over time, regardless of initial coloration, indicating UV-induced

oxidative cleavage of cellulose chains in the cotton substrate.[204,205] The magnitude of the color shift varied between samples, reflecting differences in UV-protection efficiency. ZnO-coated fabrics effectively retarded photodegradation, with EtOH_Z again showing the highest stability (ΔE = 1.5 %). In contrast, the uncoated reference exhibited substantial degradation (ΔE = 5.7 %), confirming its poor UV resistance. While UV-triggered aging was also assessed via UV–Vis spectroscopy (Section *4.4 UV-VIS analysis and UPF values*) using the same samples, this photoanalysis method provided more detailed information on both coating and substrate stability. In addition, this approach reduced inconsistencies caused by fiber or yarn heterogeneity and enabled repeated evaluation of the exact same sample area, potentially making it a more precise tool for textile-based substrates.

Table 4. Self-cleaning performance of ZnO-coated cotton samples (Blank, 0.1NaOH_30°C, 0.1NaOH_t5, EtOH_Z) showing stain degradation under solar irradiation (1 Sun) at 0, 1, 5, and 24 h intervals. Coffee (brown) and MB (blue) stains (marked with ovals) exhibit progressive fading, with RGB analysis tracking color changes over 5 h. **Publication II**; Adapted under terms of the CC-BY license.[24] Copyright 2023, The Authors, published by Elsevier B.V.

	0 h	1 h	5 h	24 h	MB	Coffee
Blank	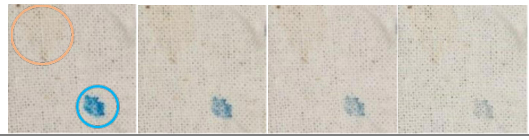				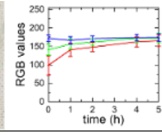	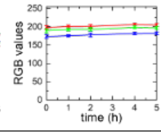
0.1NaOH_30°C	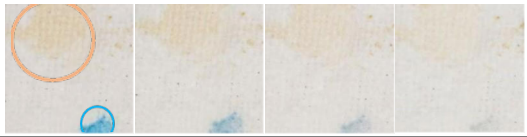				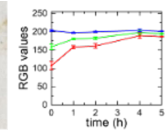	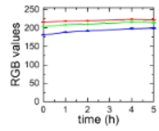
0.1NaOH_t5	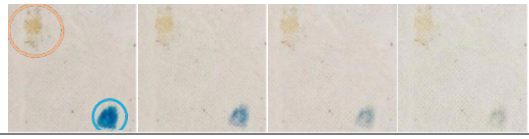				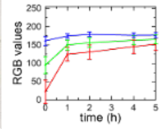	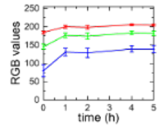
EtOH_Z					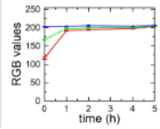	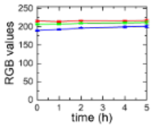

4.6 Durability testing (Publication I)

In textile applications, coating flexibility is a key factor in determining suitable placement on garments. High flexibility enables use in areas subject to frequent bending, such as underarm panels or other high-movement zones. In **Publication I**, the flexibility of the hackmanite-loaded coating was assessed using 500 flex cycles, with failure defined as visible surface breakage. Breakages were observed at two distinct points on the coated surface, although the fabric retained ease of flexing in all directions (see *Figure S7* in Publication I). The sample was also manually squeezed and bent in various ways without any issues (*Figure 14*). Taken together, these results indicate that the hackmanite-loaded coating can withstand substantial mechanical deformation, supporting its suitability even for curved substrates such as caps and visors.

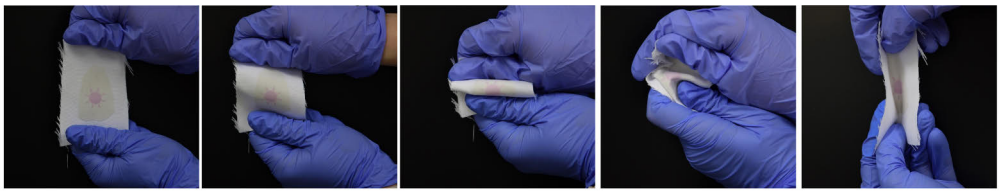

Figure 14. Photographs of the photochromic fabric during manual bending tests, with a sun-shaped pattern used as a visual indicator. **Publication I**; Adapted under terms of the CC-BY license.[22] Copyright 2024, The Authors, published by Elsevier B.V.

Washing durability is another critical factor in evaluating the suitability of functional coatings for wearable applications, since it directly relates to the garment's life cycle.[96] After five complete washing cycles, the hackmanite-coated sample lost 0.18 g (~ 3 % of its total mass; see *Table S1* in Publication I for details). The greatest mass loss occurred after the first cycle, likely due to the removal of loosely bound particles, surface dust, and residual impurities remaining from the coating process. Mass loss decreased markedly in subsequent cycles. By the fifth washing cycle, visible surface breakages had formed (see *Figure S8* in Publication I). Reflectance measurements also revealed a gradual shift in coating color toward white with each wash (*Figure 15*).

Note that withstanding five washing cycles can be considered sufficient for garments that are washed infrequently, such as caps or outdoor jackets. Durability could be further improved through additional pre-treatment steps during fabrication or by applying thinner coatings using methods like screen printing. Such strategies represent promising directions for future development.

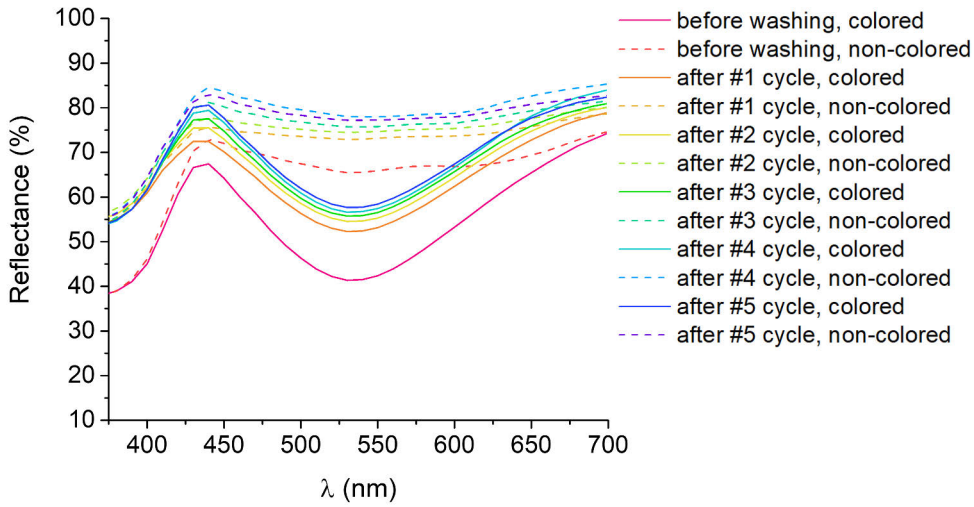

Figure 15. Reflectance measurements of the same sample before washing and after each cycle. To compare coloration changes, the coating was divided into two measurement points: colored and non-colored areas of the surface. **Publication I**; Adapted under terms of the CC-BY license.[22] Copyright 2024, The Authors, published by Elsevier B.V.

4.7 Critical analysis of photoresponsive smart textiles (Publication III)

In addition to the experimental work, this thesis provides an extensive analysis of non-electronic photoresponsive textiles from a critical perspective (**Publication III**). The first step in this analysis was to identify recurring claims related to the proposed applications of photoresponsive textiles, thereby categorizing the underlying motivations driving research in this field. To ensure comprehensive coverage of these claims, a manual assessment was performed on 130 peer-reviewed studies, selected through the procedure described in Section *3.3*. While the literature survey revealed numerous studies on self-cleaning (n = 59), photochromic (n = 32), and photothermal (n = 38) functionalities, numerical data on shape-changing (n = 0) and self-healing (n = 1) textiles were scarce or absent (see *Table S1* in Publication III). These latter features were therefore excluded from further detailed analysis in **Publication III**.

Overall, five main categories of motivations were identified: *resource saving*, *health*, *comfort*, *other reasons*, and *unspecified reasons* (see *Section 3* in Publication III for details). Among the reviewed publications, 19 % referred to sustainability or resource conservation, 28 % proposed health-related applications, and 47 % did not provide a clear justification for pursuing photoresponsive functions (*Figure 16A*) Interestingly, in research on self-cleaning textiles, the most common motivations were resource saving and health (27 % and 25 %, respectively; purple color in *Figure*

16B). Photothermal textiles (orange color in *Figure 16B*) were more frequently associated with health-related applications (38 %), with less emphasis on comfort (26 %) or resource saving (23 %). For photochromic textiles (yellow color in *Figure 16B*), a considerable share was developed for health-related purposes, while as many as 72 % of the studies offered no explicit motivation for this line of research. As shown in Figure *16B*, percentages may exceed 100 % because several studies reported more than one motivational factor.

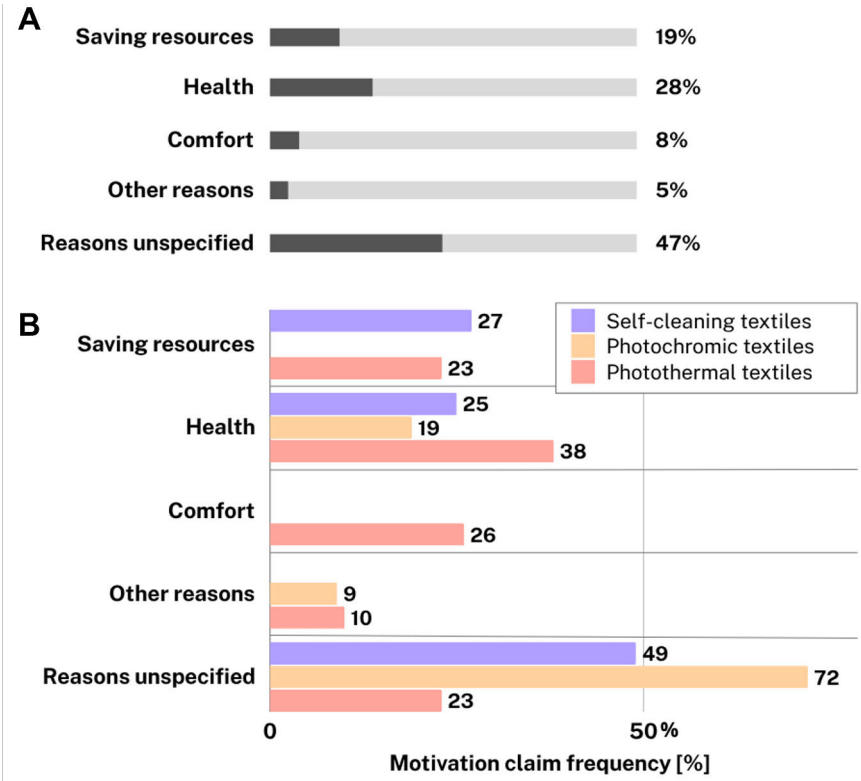

Figure 16. Percentage distribution of research motivations in the reviewed articles. **(A)** Combined results for all sections (*n = 130*). **(B)** Distribution by functionality: self-cleaning/photocatalysis (*n = 59*; purple), photochromic (*n = 32*; yellow), and photothermal (*n = 38*; orange). Percentages may exceed 100 % as several studies reported multiple motivational factors. **Publication III**; *Manuscript submitted*.

Note that based on these results, **Publication III** provides a detailed, feature-oriented analysis assessing how the reported claims were justified and delivered in each publication. For example, it evaluates the light sources used in most of the reviewed studies, identifying which realistically simulate outdoor or indoor lighting conditions, as well as the timescales required to achieve a

photoresponsive effect, sometimes extending to several days (e.g., self-cleaning textiles in[140]). The purpose of this section in the thesis is to cover the most significant observations from that analysis to highlight their main limitations and performance challenges of non-electronic photoresponsive textiles. These challenges can be broadly grouped into three categories: dependence on specific light parameters (Section *4.7.1*), insufficiently validated sustainability claims (Section *4.7.2 Sustainability claims*), and mechanical durability and end-of-life considerations, including recyclability (Section *4.7.3 Mechanical, durability and recycling challenges*).

4.7.1 Dependence on specific light parameters

The first and perhaps the most important limitation in application of photoresponsive textiles is their dependence on specific light parameters, which are rarely replicated in practical outdoor settings. The performance of photoresponsive materials is strongly influenced by both light intensity and wavelength, with insufficient illumination often reducing or completely preventing the intended response. Laboratory testing frequently employs solar simulators (e.g., AM1.5 spectrum), which can accelerate exposure by approximately tenfold—1,000 hours of simulated light representing about one year of outdoor exposure.[206,207] Although such controlled exposure is valuable for rapid performance assessments or aging tests, it does not capture the variability of real lighting conditions, which are shaped by factors such as weather, season, and geographic location.[208] The problem arises when a textile demonstrates functionality only under accelerated conditions but fails to perform in its intended environment.

The gap between laboratory conditions and actual environments become even more pronounced when targeting indoor applications. For example, compact fluorescent lamps commonly used indoors emit primarily visible light (400–800 nm) at irradiance intensities below 30 W m^{-2}, whereas laboratory solar simulators deliver full-spectrum output (300–4,000 nm) at 1,000 W m^{-2}. Not to limit this discussion only to certain light source, Figure *17* presents the general variation in illuminance across different settings using lux values. Illuminance in typical households ranges from less than 50 lux in shaded areas to about 1,000 lux near windows on bright days, dropping to 10–200 lux at night. Hospital environments, often cited in studies of photocatalytic and photothermal textiles for antimicrobial purposes, show similar variability. Patient rooms typically maintain 50–300 lux, while window-adjacent areas vary seasonally between 100–1,000 lux.[209–211] Only surgical theaters approach outdoor-like intensities, with artificial lighting levels of 10,000–160,000 lux, comparable to direct sunlight at ~ 100,000 lux.[212]

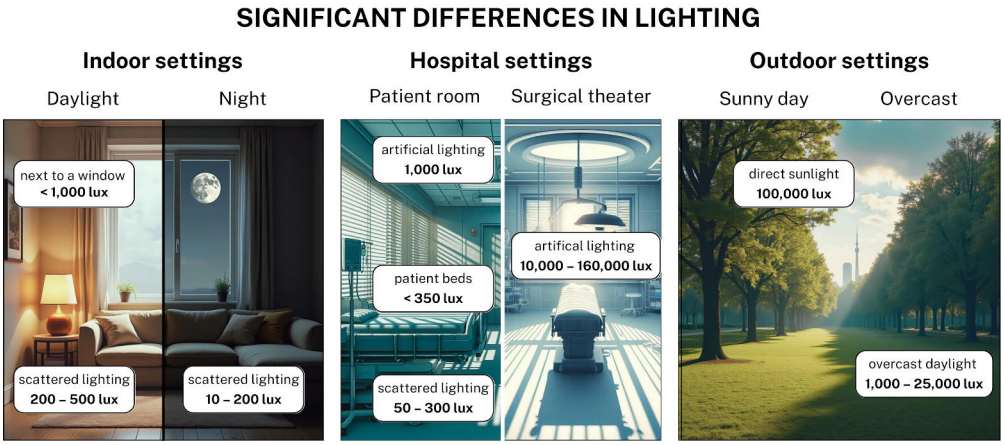

Figure 17. Schematic illustration of typical illuminance values (in lux) across different environments: from dim indoor spaces to bright daylight (*left*), clinical settings such as patient rooms and surgical theatres (*middle*), and natural outdoor conditions (*right*). These variations in illuminance strongly affect the performance of photoresponsive materials by determining their activation thresholds. **Publication III***; Manuscript submitted.*

UV-dependent functionalities face particular limitations indoors, since most artificial lighting contains little to no UV radiation. In such cases, both light intensity and spectral composition are insufficient to activate the intended response. As a result, textiles that perform well under direct sunlight may show negligible or no functionality in indoor settings. For example, self-cleaning textiles based on UV-active photocatalytic materials are unlikely to undergo photocatalysis (i.e., self-cleaning) indoors.[43] Similarly, photothermal garments intended to provide localized heating as an energy-efficient alternative to heating, ventilation, and air conditioning (HVAC) systems is ineffective under indoor lighting, where irradiance is orders of magnitude lower and the spectrum differs significantly from that of laboratory light sources.[182]

While specialized lamps could theoretically address this limitation, using UV lamps or solar simulators to clean and heat garments is neither practical nor energy efficient. It should be emphasised that indoor artificial lighting already accounts for 6 % to nearly 20 % of total building energy use,[213,214] and adding more energy-intensive lamps would directly conflict with the goal of reducing energy consumption, especially when such textiles are promoted as resource-saving solutions (see more in Section *4.7.2*).

On a positive note, self-cleaning textiles (both photocatalysis- and photothermal-based) could still be effective in healthcare environments, where cleanliness is a priority and specialized light sources (e.g., UV or Near-infrared (NIR) lamps) are already used for disinfection. Such materials could be particularly valuable during

pandemics or wartime, when supply shortages increase the need for reusable, low-maintenance fabrics.[215] Other promising examples include photochromic textiles, which require only brief light exposure to change color and can function effectively across diverse conditions. UV-monitoring textiles have already been shown to work reliably outdoors, provided that visible light does not interfere with coloration.[22,23,96] Therefore, considering the intended application environment of photoresponsive textiles at the earliest stages of development would be one important step toward enhancing their practical applicability.

4.7.2 Sustainability claims

As shown in Figure *16A*, 19 % of the reviewed studies identified resource saving as the primary motivation for developing photoresponsive textiles. Indeed, as discussed already in Section *1*, non-electronic photoresponsive materials hold considerable potential for contributing to sustainability, just because they utilise an abundant energy source to deliver functions that would otherwise require electricity. Besides that, the environmental benefits claimed for such textiles take several other forms. For example, photocatalytic fabrics could reduce washing frequency, thereby saving water and energy, but also limiting the release of microplastics and detergents into water streams, and reducing the human labor required for the washing process.[25,26,43,177,178] Self-disinfecting fabrics (both photocatalytic and photothermal) could extend the lifespan of single-use products, lowering plastic or hospital waste.[160,216] Photothermal textiles could help lower electricity consumption by providing localized heating (see Section *4.7.1*), while also enhancing comfort in remote or cold environments where reliance on external energy sources could be limited.[157,181–183] However, as discussed earlier in this section, the effectiveness of these solutions depends heavily on light conditions with many photoresponsive functions requiring high-intensity or wavelength-specific illumination. If the available light is insufficient to activate the functionality, the material cannot deliver the promised performance and therefore cannot achieve the claimed benefits.

For example, the most frequently claimed benefit of self-cleaning textiles is resource savings achieved through less frequent washing. The fact is that laundry itself is highly resource intensive. Globally, domestic washing consumes about 20 billion cubic meters of freshwater annually, while in the European Union alone, energy use from laundering was estimated at 35 TWh in 2005.[178,217] Moreover, washing is one of the main sources of microplastic pollutions in ecosystems. If self-cleaning textiles could reliably reduce its frequency, the potential savings would be substantial. Yet, their performance has most often been evaluated under controlled and intense lighting conditions (using e.g., strong artificial sunlight), that is far from

what is encountered in daily life (see Section *3.2.1* in Publication III for more details).

Notably in this case, lighting may not be the only limitation. Even if such garments reached the market, consumer acceptance remains uncertain. Many people are accustomed to quick, machine-based cleaning cycles and may not be willing to leave clothes outside for several days, and only in sunny conditions, to achieve similar results, especially for garments washed frequently. Research by Klepp *et al*.[218] shows that 39 % of surveyed users wash or dry-clean clothing after every wear, while 14 % do so after every second wear. T-shirts, for example, are washed an average of 150 times across 151 wears. To benefit from self-cleaning properties, users would need to replace regular laundering with outdoor exposure, which requires both suitable weather conditions and access to outdoor space. Such behavioral changes demand considerable effort, and it remains doubtful whether people will readily adapt their routines.

More realistic applications may be found in contexts where longer exposure is acceptable, such as outdoor clothing, delicate fabrics (e.g., silk), or indoor items like couch cushions, which are washed infrequently (see Section *2.3.2*). The same research[218] shows that coats (e.g., winter jackets) are washed only 8 times despite being worn 257 times, partly because oversized garments are more difficult to wash. However, without proper maintenance, these items often lose their appearance, leading to premature disposal or reduced use to avoid damage. In such cases, long-term exposure to sunlight might be preferable to buying a replacement simply because of stains.[141,142] Nonetheless, these claims remain speculative, as none of the reviewed studies provided sufficient evidence to confirm them. Therefore, while photoresponsive textiles are often presented as offering sustainability benefits, it remains unclear whether these claims can be translated into measurable impacts under realistic use conditions.

4.7.3 Mechanical, durability and recycling challenges

Once photoresponsive textiles become more adopted to perform in intended settings, their further development challenge will be ensuring that they maintain functionality under everyday mechanical stress, withstand repeated washing, and remain recyclable once their service life ends. At present, most smart textiles are still at low technology readiness levels, with research focused mainly on proof-of-concept rather than market-ready products. Consequently, aspects such as durability and recyclability are often postponed to later stages of development. For instance, within this thesis, washing resistance was evaluated in **Publication I** but not in **Publication II**, while recycling was not addressed in either case. However, to

prepare lab-based prototypes for large-scale manufacturing, it is becoming increasingly important to align research conditions with industrial practices.

In industry, textiles are routinely subjected to standardized mechanical tests, and lab-scale prototypes should likewise undergo comparable evaluations to assess their durability and usability. Encouragingly, nearly half of the reviewed studies (48 %; see Supporting Information in Publication III) included some form of mechanical testing, which is a relatively high proportion given that many smart textile studies remain at low readiness levels. By contrast, testing for laundering durability remains far less common. Repeated washing exposes textiles to mechanical agitation, detergents, and heat, which can not only degrade photoresponsive performance but also accelerate the release of NPs or other active components into wastewater. Such leaching poses environmental concerns due to the uncertain toxicity of many NPs, yet this issue is rarely addressed. Only 30 % of the reviewed publications evaluated washing durability using standardized methods (Supporting Information in Publication III). The available results consistently show that washing reduces the durability of functional coatings, with performance declining across successive cycles. Thus, if smart textiles become widespread, technical solutions such as washing machine filters designed to capture NPs may be required to limit environmental release.

Recycling is another aspect that is too often overlooked, which could actually pose a serious challenge for future textile recovery systems. At present, only about 1 % of textile waste is recovered in closed-loop processes within the EU, largely due to technical limitations.[219] Separating embedded active compounds from textile substrates is even more complex,[20] making it likely that smart textiles will be incinerated or landfilled at the end of their service life. In such cases, any potential environmental benefits of photoresponsive textiles risk being outweighed by their end-of-life impact—assuming they even reach the market in the first place. With new EU regulations pushing for circular recovery solutions,[219] even the best-performing photoresponsive textiles are unlikely to be commercialised without a clear and feasible recycling strategy. The consistent lack of attention to end-of-life management across the reviewed studies highlights a major gap that must be addressed if photoresponsive textiles are to become both commercialized and sustainable.

5 Conclusions

The first main objective of this thesis was to develop circuit-free smart textiles that rely solely on light to deliver advanced functions, with a focus on photochromic and photocatalytic properties. These textiles were fabricated using coating-based approaches, chosen for their simplicity, cost-effectiveness, and potential scalability. Color-changing textiles were developed using the photochromic mineral hackmanite (**Publication I**), which was successfully coated onto a textile substrate for the first time, while photocatalytic textiles were synthesised through microwave-assisted in-situ growth of ZnO flower-like crystals on cotton (**Publication II**).

Among potential applications, photochromic textiles proved particularly suitable for UV monitoring. With melanoma rates increasing and public awareness of sun exposure risks often insufficient, wearables that visually alert users to harmful UV levels are highly relevant. For **Publication I**, hackmanite was chosen as the photochromic material due to its strong UV-responsive color change and its activation threshold, which closely aligns with the erythemal action spectrum of human skin. It was applied to synthetic textiles using a scalable doctor blade coating method with a formulation free of hazardous compounds, ensuring suitability for skin contact. One important finding was that the coating achieved strong coloration with only a small amount of hackmanite, while using a coating method instead of spin-based techniques avoided potential damage to the structural integrity of the yarn. The coated fabric detected UVI levels below 3, the limit at which preventive measures are recommended to avoid early sunburn. Moreover, the hackmanite-coated samples maintained stable color saturation over 20 photochromic cycles and withstood five washing and 500 flex cycles before surface degradation occurred. Together, these results highlight the practical potential of hackmanite-based coatings for accessories such as caps, which are washed infrequently.

Photocatalytic textiles formed the second focus of this thesis, motivated by their potential to reduce laundry frequency and resource consumption. In **Publication II**, ZnO was selected as the photocatalytic (i.e., self-cleaning and UV-blocking) material owing to its biocompatibility, low toxicity, and strong photocatalytic activity. The efficiency of ZnO is highly dependent on its crystal morphology, with flower-like structures reported as the most effective. The novelty of **Publication II** was the

systematic analysis of synthesis protocols to understand and determine optimal coating conditions for textiles. Nine parameters, including solvent type, precursor type, concentration, and synthesis duration, were investigated for their influence on ZnO crystal morphology and resulting photoresponsive efficiency. The fabricated ZnO-coated cotton samples demonstrated nearly complete UV blocking (confirmed by UPF values) and effective self-cleaning, successfully removing stains such as coffee and MB. The most efficient coatings achieved 73 % MB degradation within 1 h and 90 % after 24 h of 1 Sun exposure under low RH (10 %).

The promising outcomes of both publications highlight opportunities to further refine the prototypes obtained in both **Publications I** and **II**. In **Publication I**, the photochromic fabric was confirmed to respond effectively to relevant UV doses, consistent with standardized UVI values. One important consideration, however, is that in hackmanite both coloration and bleaching are triggered by wavelengths abundant in the solar spectrum, with intense visible light quickly erasing the color. This, incorporating a switchable filter that selectively absorbs UV and visible wavelengths into the design, could be a promising next step in advancing photochromic textiles. In **Publication II**, the self-cleaning performance of ZnO-coated textiles was assessed using not only MB but also a common stain, coffee. Laboratory experiments conducted under high light intensity produced positive results within just the first hour of exposure, indicating promising potential for outdoor use. Further research into the practical application of these self-cleaning textiles in various environments would be an interesting area to explore. For example, developing coatings that activate photocatalysis under shorter light exposures could greatly broaden their range of applications. Finally, more extensive durability testing and improved coating adhesion to textile substrates in both **Publications I** and **II** would support longer lifecycles and enhance overall performance. These aspects were also addressed in the assessment done in **Publication III**, with the results complementing the experimental work presented in this thesis.

The main purpose of the analysis conducted in **Publication III** was to evaluate whether the frequently claimed advantages of non-electronic photoresponsive textiles can realistically be achieved under intended usage conditions. While many proposed applications appeared promising, they often proved impractical when laboratory results under idealized settings were compared with real-world use contexts in which such textiles would be used. Consequently, many of the reported environmental benefits and performance promises simply lacked measurable validation.

It was particularly noted that many studies tested samples under light intensities far higher than those normally encountered indoors, even though most proposed applications were designed for indoor use. In many study cases, solar simulators

producing radiation 100 to 10,000 times stronger than typical indoor illumination were used to evaluate photoresponsive performance of smart textiles intended for indoor applications. For example, photothermal garments promoted as energy-saving alternatives to HVAC systems appear effective when tested with simulated sunlight but are unlikely to provide meaningful heating indoors. Likewise, UV-driven self-cleaning textiles that perform under intense, wavelength-specific artificial light will rather fail to work under indoor conditions, where irradiance is much lower and UV radiation is nearly absent. In short, functionalities demonstrated only under idealized laboratory conditions cannot be expected to operate reliably in everyday use, specifically indoors, undermining performance claims and associated sustainability benefits.

Another recurring issue concerns durability testing, recycling strategies, and even consumer acceptance. Assessments of washing, eco-design and life-cycle considerations were limited or missing in many studies, including this thesis, even though sustainability was often cited as a primary research motivation. It is understandable that such studies are rarely conducted at low technology readiness levels, as seen in the experimental case studies here, particularly in the development of self-cleaning structures. Yet, at later development stages such assessments are essential for determining textile longevity and, ultimately, their environmental impact.

These observations raise important (and somewhat provocative) questions: Is sustainability too often unjustifiably cited as a key motivation for research on photoresponsive textiles? And how should such claims be fairly evaluated? Self-cleaning fabrics provide an interesting example. While they could in theory reduce washing frequency, their reliance on outdoor use, long exposure times, and specific lighting conditions makes it unlikely that consumers would abandon established laundry habits. More realistic applications may be found in contexts where longer exposure is acceptable, such as outdoor gear, delicate fabrics like silk, or indoor furnishings that are washed infrequently. In such cases, where garments might otherwise be discarded when soiled rather than washed, self-cleaning textiles could genuinely contribute to resource savings. Nevertheless, these potential scenarios still require thoughtful evaluation.

Despite their uncertain benefits in sustainability contexts, photoresponsive textiles still offer strong promise in other areas, particularly health-related applications. For example, properly designed photochromic UV-sensing textiles can function effectively in outdoor lighting, identifying relevant UV dosage linked to health hazards. Similarly, light-driven self-disinfecting materials (both photocatalytic and photothermal) could be valuable in healthcare settings, where specialized lamps are already routinely used for sterilization, and any extra

protection against microbes is especially beneficial during shortages, such as pandemics or wars.

In summary, this thesis has demonstrated that light alone can power key smart functions in textiles, transforming conventional garments into tools that can enhance daily life. The experimental results presented here open pathways toward sustainable, circuit-free materials with applications in UV sensing and self-cleaning. The broader critical analysis of non-electronic photoresponsive textiles further emphasized that their transition from laboratory prototypes to practical adoption depends on validation under realistic conditions. Only through such verification can these materials deliver the benefits claimed for their intended applications.

Acknowledgements

The research presented in this thesis was carried out between 2021 and 2025 in the Solar Energy Materials and Systems group at the Materials Engineering Unit, University of Turku. Part of the work for Publication I was conducted in the laboratory of the Intelligent Materials Chemistry Group, Department of Chemistry, University of Turku, and at the Center for Creative Industries & Professions, VIA University College, Herning, Denmark. I gratefully acknowledge the Materials Research Infrastructure (MARI) and especially the Department of Physics and Astronomy, University of Turku, for access to and support with the SEM and BIB facilities, which were essential for Publications I and II. I also warmly thank Erasmus+ and the Faculty of Technology for supporting my research mobility, as well as TOP-Säätiö for financial support. Finally, I acknowledge NordForsk for funding the project *Nordic Network on Smart Light-Conversion Textiles Beyond Electric Circuits* (project number 103894).

I sincerely thank my supervisor, Professor Kati Miettunen, for her approachable and supportive guidance. She encouraged me to participate in conferences and learning opportunities, which helped me expand my network, collaborate with excellent researchers, and grow as a scientist. I am also very grateful to Dr. Emilia Palo, whose academic and personal support during my doctoral studies was invaluable. She gave me the confidence to apply for external funding, guided me through publication processes, reviewed my presentations, and was always available whenever I needed advice.

I extend my warm thanks to Professor Mika Lastusaari from the Intelligent Materials Chemistry Group at the University of Turku for his support with hackmanite. Without him, a central part of this thesis would not have been possible. I am equally thankful to Dr. Sami Vuori for his continuous support, from the earliest stages of Publication I through many aspects of my doctoral journey. His advice and assistance were invaluable, and I could not have asked for a better lab buddy.

I am very thankful to Dr. Anne Louise Bang, Poul-Erik Jørgensen, Mathias Winther, Dr. Malene Harsaae, Lena Kramer Pedersen, and Inger Marie Ladekarl for their kind hospitality during my stay at VIA University College in Herning, Denmark. I also thank Professor Jaana Vapaavuori, whose contribution was vital to

Publication III. She is the reason I chose the doctoral path. Before starting my research in Turku, I had the privilege of working with her Multifunctional Materials Design group at Aalto University. I am grateful as well to Professor Delia Dumitrescu from the University of Borås, Sweden, whose prototypes of photochromic samples influenced the work in Publication I, and to Professor Marjan Kooroshnia from the University of Borås, with whom I continued to explore hackmanite-coated textiles.

I warmly thank my co-author, fellow doctoral researcher Rustem Nizamov, for his valuable insights in Publication II. I also appreciate the contributions of all colleagues involved in Publications I–III, including those not listed as co-authors. Their advice, discussions, and analytical skills greatly supported this work. In particular, I thank Dr. Hannah Byron, Dr. Heikki Palonen, Dr. Janne Halme, and Zahra Madani—without their help, this thesis would not be the same. I am grateful to Dr. Ermei Mäkilä and Dr. Sari Granroth for their assistance with SEM measurements, and to Mikael for his willingness to help with technical challenges. My thanks also go to the lab engineering team (Akseli, Teemu, Helen) for their technical support and the many shared coffee breaks. I am also thankful to Dr. Manish Kumar for his help in applying for funding and for the uplifting coffee breaks, and to everyone from the old library floor for the friendly chats on my way to lunch.

I am especially thankful to Maryam, who shared the early years of my doctoral journey at the University of Turku, and to Mahdi, who was always there with his amazing smile. I am also grateful to Ransell and Tomasz for always being there to spill the tea. To Matteo, with whom I explored smart textiles beyond academia; to Petra, who accepted my weirdness. And to Giulnara, who kept everything well organized and patiently managed my often-delayed emails. To my Polish friends, especially Magda and Kasia, who made me feel as though I was still a little bit in Poland.

My deepest thanks go to Juuso, the most amazing person, who supported me through this PhD and in life overall. I also thank my two fluffy cats, who always let me put my face in their bellies when I needed to calm down.

Finally, I warmly thank my dear family and friends in Poland for their unwavering emotional support throughout the years I have spent away from home. *Dla mojej Mamy, która zawsze przy mnie była, nawet wtedy, gdy musiała przeznaczyć całą swoją siłę na walkę z chorobą. Oraz dla mojego Taty, który na pewno jest teraz bardzo szczęśliwy.*

Turku, 29.08.2025
Alicja Ławrynowicz

List of References

[1] S. A. Behera, S. Panda, S. Hajra, K. R. Kaja, A. K. Pandey, A. Barranco, S. M. Jeong, V. Vivekananthan, H. J. Kim, P. G. R. Achary, *Adv. Sustain. Syst.* **2024**, *8*, 2400344.

[2] P. Veske, E. Ilén, *J. Text. Inst.* **2021**, *112*, 1500.

[3] J. Li, H. Wang, H. Mao, L. Li, J. Shi, H. Shi, *Sol. Energy Mater. Sol. Cells* **2020**, *217*, 110704.

[4] S. Qiu, H. Jia, S. Jiang, *Mater. Lett.* **2021**, *300*, 130217.

[5] S. Rotzler, M. Von Krshiwoblozki, C. Kallmayer, M. Schneider-Ramelow, *Adv. Funct. Mater.* **2025**, *35*, 2417344.

[6] Y. Wu, S. S. Mechael, T. B. Carmichael, *Acc. Chem. Res.* **2021**, *54*, 4051.

[7] C. Wang, L. Fu, D. S. Ametefe, S. Wang, D. John, *Neural Comput. Appl.* **2025**, *37*, 2089.

[8] I. Ali, M. Dulal, N. Karim, S. Afroj, *Small Struct.* **2024**, *5*, 2300282.

[9] B. Garnier, P. Mariage, F. Rault, C. Cochrane, V. Koncar, *Smart Mater. Struct.* **2020**, *29*, 085017.

[10] F. Mokhtari, G. M. Spinks, C. Fay, Z. Cheng, R. Raad, J. Xi, J. Foroughi, *Adv. Mater. Technol.* **2020**, *5*, DOI 10.1002/admt.201900900.

[11] Q. Shi, J. Sun, C. Hou, Y. Li, Q. Zhang, H. Wang, *Adv. Fiber Mater.* **2019**, *1*, 3.

[12] E. Ilén, J. Halme, E. Palovuori, B. Blomstedt, F. Elsehrawy, *Sun-Powered Textiles: Designing Energy-Autonomous Electro-Textile Systems with Solar Cells*, Aalto University, Espoo, **2022**.

[13] K. Miettunen, M. Hadadian, J. V. García, A. Lawrynowicz, E. Akulenko, O. J. Rojas, M. Hummel, J. Vapaavuori, *WIREs Energy Environ.* **2024**, *13*, e508.

[14] M. L. R. Liman, M. T. Islam, *J. Mater. Chem. A* **2022**, *10*, 2697.

[15] European Commission, "Circular economy for textiles: taking responsibility to reduce, reuse and recycle textile waste and boosting markets for used textiles," **n.d.**

[16] W. Li, H. Zhang, T. Chen, L. Yang, C. Sheng, H. Wu, N. Mao, *Text. Res. J.* **2022**, *92*, 739.

[17] M. T. Abate, S. Seipel, J. Yu, M. Viková, M. Vik, A. Ferri, J. Guan, G. Chen, V. Nierstrasz, *Dyes Pigments* **2020**, *183*, 108671.

[18] Y.-M. Cao, M. Zheng, Y.-F. Li, W.-Y. Zhai, G.-T. Yuan, M. Zheng, M.-P. Zhuo, Z.-S. Wang, L.-S. Liao, *ACS Appl. Mater. Interfaces* **2021**, *13*, 48988.

[19] M. van Aubel, *Solar Future: How to Design a Post-Fossil World with the Sun*, Jap Sam Books, And Made Possible With The Support Of Creative Fund NL, Prins Bernhard Cultuurfonds And The Sandberg Institute., **n.d.**

[20] M. Dulal, S. Afroj, M. R. Islam, M. Zhang, Y. Yang, H. Hu, K. S. Novoselov, N. Karim, *Small* **2024**, *20*, 2407207.

[21] W. Fang, E. Sairanen, S. Vuori, M. Rissanen, I. Norrbo, M. Lastusaari, H. Sixta, *ACS Sustain. Chem. Eng.* **2021**, *9*, 16338.

[22] A. Lawrynowicz, S. Vuori, E. Palo, M. Winther, M. Lastusaari, K. Miettunen, *Chem. Eng. J.* **2024**, *494*, 153069.

[23] Y. Zheng, W. Panatdasirisuk, J. Liu, A. Tong, Y. Xiang, S. Yang, *Adv. Mater. Technol.* **2020**, *5*, 2000564.

[24] A. Lawrynowicz, E. Palo, R. Nizamov, K. Miettunen, *J. Photochem. Photobiol. Chem.* **2024**, *450*, 115420.

[25] Z. Qi, K. Wang, J. Chen, D. Gao, Y. Ren, C. Wang, *New J. Chem.* **2021**, *45*, 11119.
[26] H. Zhao, S. Wang, M. Zhou, Z. Cai, Y. Zhao, *J. Mater. Sci. Mater. Electron.* **2022**, *33*, 24706.
[27] Y. Zhang, X. Xia, K. Ma, G. Xia, M. Wu, Y. H. Cheung, H. Yu, B. Zou, X. Zhang, O. K. Farha, J. H. Xin, *Adv. Funct. Mater.* **2023**, *33*, DOI 10.1002/adfm.202301607.
[28] T. V. Pinto, D. M. Fernandes, A. Guedes, N. Cardoso, N. F. Durães, C. Silva, C. Pereira, C. Freire, *Chem. Eng. J.* **2018**, *350*, 856.
[29] H. Zhang, J. Fan, H. Cheng, D. Yu, W. Wang, *Surf. Interfaces* **2024**, *51*, 104795.
[30] Y.-F. Chen, M.-R. Huang, Y.-S. Hsu, M.-H. Chang, T.-Y. Lo, B. Gautam, H.-H. Hsu, J.-T. Chen, *ACS Appl. Mater. Interfaces* **2024**, *16*, 29153.
[31] R. R. Ruckdashel, D. Venkataraman, J. H. Park, *J. Appl. Phys.* **2021**, *129*, DOI 10.1063/5.0024006.
[32] S.-Y. Fu, X.-Q. Feng, B. Lauke, Y.-W. Mai, *Compos. Part B Eng.* **2008**, *39*, 933.
[33] V. Malm, M. Strååt, P. Walkenström, *Text. Res. J.* **2014**, *84*, 125.
[34] M. Aldib, R. M. Christie, *Color. Technol.* **2011**, *127*, 282.
[35] Y. Ma, Y. Zou, Z. Zhang, J. Fang, W. Liu, Y. Ni, L. Fang, C. Lu, Z. Xu, *Cellulose* **2020**, *27*, 561.
[36] J. Chen, X. Chen, U. Azhar, X. Yang, C. Zhou, M. Yan, H. Li, C. Zong, *Chem. Eng. J.* **2023**, *466*, 143176.
[37] C. Yang, J. Wang, J. Li, H. Zhang, C. Shi, Z. Guo, B. Bai, *Prog. Org. Coat.* **2021**, *160*, 106520.
[38] Y. Yang, M. Li, S. Fu, *Prog. Org. Coat.* **2021**, *158*, 106348.
[39] D. K. Macharia, S. Ahmed, B. Zhu, Z. Liu, Z. Wang, J. I. Mwasiagi, Z. Chen, M. Zhu, *ACS Appl. Mater. Interfaces* **2019**, *11*, 13370.
[40] S. Seipel, J. Yu, M. Viková, M. Vik, M. Koldinská, A. Havelka, V. A. Nierstrasz, *Fibers Polym.* **2019**, *20*, 1424.
[41] H. Yang, P. Jiang, *Langmuir* **2010**, *26*, 12598.
[42] S. Lee, S. Park, *RSC Adv.* **2024**, *14*, 40098.
[43] Z. Moridi Mahdieh, S. Shekarriz, F. Afshar Taromi, *Clean Technol. Environ. Policy* **2022**, *24*, 2143.
[44] Y. L. Lam, C. W. Kan, C. W. M. Yuen, *Cellulose* **2011**, *18*, 493.
[45] J. Budd, T. M. Herrington, *Colloids Surf.* **1989**, *36*, 273.
[46] S. Kalia, B. S. Kaith, I. Kaur, *Polym. Eng. Sci.* **2009**, *49*, 1253.
[47] A. Montarsolo, R. Mossotti, R. Innocenti, E. Vassallo, *Surf. Coat. Technol.* **2013**, *224*, 109.
[48] In *Join. Technol.*, InTech, **2016**.
[49] Ç. Akduman, N. Oğlakcıoğlu, A. Çay, *Polym. Eng. Sci.* **2024**, *64*, 5360.
[50] R. Rodriguez, D. G. Bekas, S. Flórez, M. Kosarli, A. S. Paipetis, *Polymer* **2020**, *187*, 122084.
[51] Z. He, B. Bao, J. Fan, W. Wang, D. Yu, *Colloids Surf. Physicochem. Eng. Asp.* **2020**, *594*, 124661.
[52] L. Si, Y. Zhang, Y. Yin, C. Wang, *Prog. Org. Coat.* **2021**, *151*, 106080.
[53] E. Gibertini, F. Carosio, K. Aykanat, A. Accogli, G. Panzeri, L. Magagnin, *Surf. Interfaces* **2021**, *25*, 101252.
[54] R. Pardo, M. Zayat, D. Levy, *J. Photochem. Photobiol. Chem.* **2008**, *198*, 232.
[55] T. Yimyai, D. Crespy, A. Pena-Francesch, *Adv. Funct. Mater.* **2023**, *33*, DOI 10.1002/adfm.202213717.
[56] M. Nemiwal, D. Kumar, *Inorg. Chem. Commun.* **2021**, *128*, 108602.
[57] Q. Liao, Y. Yin, J. Zhang, W. Si, W. Hou, L. Qin, *Int. J. Mol. Sci.* **2022**, *23*, 13236.
[58] S. Mura, G. Greppi, L. Malfatti, B. Lasio, V. Sanna, M. E. Mura, S. Marceddu, A. Lugliè, *J. Colloid Interface Sci.* **2015**, *456*, 85.
[59] S. Ashoka, G. Nagaraju, C. N. Tharamani, G. T. Chandrappa, *Mater. Lett.* **2009**, *63*, 873.
[60] R. Shi, P. Yang, X. Dong, Q. Ma, A. Zhang, *Appl. Surf. Sci.* **2013**, *264*, 162.
[61] Y. Fang, Z. Li, S. Xu, D. Han, D. Lu, *J. Alloys Compd.* **2013**, *575*, 359.
[62] M. Z. Khan, V. Baheti, J. Militky, J. Wiener, A. Ali, *J. Ind. Text.* **2020**, *50*, 543.

[63] X. Zou, J. Ke, J. Hao, X. Yan, Y. Tian, *Phys. B Condens. Matter* **2022**, *624*, 413395.
[64] L. Zhu, Y. Li, W. Zeng, *Appl. Surf. Sci.* **2018**, *427*, 281.
[65] V. H. Tran Thi, B.-K. Lee, *J. Photochem. Photobiol. Chem.* **2017**, *338*, 13.
[66] K. U. Rahman, E. P. Ferreira-Neto, G. U. Rahman, R. Parveen, A. S. Monteiro, G. Rahman, Q. Van Le, R. R. Domeneguetti, S. J. L. Ribeiro, S. Ullah, *J. Environ. Chem. Eng.* **2021**, *9*, 104708.
[67] S. Vuori, H. Byron, I. Norrbo, M. Tuomisto, M. Lastusaari, *J. Ind. Eng. Chem.* **2023**, *120*, 361.
[68] S. Fan, Y. Lam, J. Yang, X. Bian, J. H. Xin, *Surf. Interfaces* **2022**, *34*, 102383.
[69] P. Colinet, H. Byron, S. Vuori, J.-P. Lehtiö, P. Laukkanen, L. Van Goethem, M. Lastusaari, T. Le Bahers, *Proc. Natl. Acad. Sci.* **2022**, *119*, e2202487119.
[70] I. Norrbo, A. Curutchet, A. Kuusisto, J. Mäkelä, P. Laukkanen, P. Paturi, T. Laihinen, J. Sinkkonen, E. Wetterskog, F. Mamedov, T. Le Bahers, M. Lastusaari, *Mater. Horiz.* **2018**, *5*, 569.
[71] Y. Qi, J. Fan, Y. Chang, Y. Li, B. Bao, B. Yan, H. Li, P. Cong, *Dyes Pigments* **2021**, *193*, 109507.
[72] J. Fan, B. Bao, Z. Wang, H. Li, Y. Wang, Y. Chen, W. Wang, D. Yu, *Chem. Eng. J.* **2021**, *404*, 126488.
[73] S. Nigel Corns, S. M. Partington, A. D. Towns, *Color. Technol.* **2009**, *125*, 249.
[74] A. Abdollahi, A. Mouraki, M. H. Sharifian, A. R. Mahdavian, *Carbohydr. Polym.* **2018**, *200*, 583.
[75] M. Mandal, D. Banik, A. Karak, S. K. Manna, A. K. Mahapatra, *ACS Omega* **2022**, *7*, 36988.
[76] X. Shen, M. Ge, Y. Jin, *J. Lumin.* **2022**, *252*, 119373.
[77] P. Lu, D. Ahn, R. Yunis, L. Delafresnaye, N. Corrigan, C. Boyer, C. Barner-Kowollik, Z. A. Page, *Matter* **2021**, *4*, 2172.
[78] A. Subaihi, S. D. Al-Qahtani, R. M. S. Attar, K. Alkhamis, H. K. Alzahrani, M. Alhasani, N. M. El-Metwaly, *Cellulose* **2022**, *29*, 6393.
[79] T. Zheng, Z. Xu, Y. Zhao, H. Li, R. Jian, C. Lu, *Sens. Actuators B Chem.* **2018**, *255*, 3305.
[80] J. Fan, B. Bao, Z. Wang, R. Xu, W. Wang, D. Yu, *Cellulose* **2020**, *27*, 493.
[81] K. E. Overdahl, C. D. Kassotis, K. Hoffman, G. J. Getzinger, A. Phillips, S. Hammel, H. M. Stapleton, P. L. Ferguson, *Environ. Pollut.* **2023**, *337*, 122491.
[82] M. Punzi, A. Anbalagan, R. Aragão Börner, B.-M. Svensson, M. Jonstrup, B. Mattiasson, *Chem. Eng. J.* **2015**, *270*, 290.
[83] L. Da Silva Leite, B. De Souza Maselli, G. De Aragão Umbuzeiro, R. F. Pupo Nogueira, *Chemosphere* **2016**, *148*, 511.
[84] Y. Badour, V. Jubera, I. Andron, C. Frayret, M. Gaudon, *Opt. Mater. X* **2021**, *12*, 100110.
[85] C. Agamah, S. Vuori, P. Colinet, I. Norrbo, J. M. De Carvalho, L. K. Okada Nakamura, J. Lindblom, L. Van Goethem, A. Emmermann, T. Saarinen, T. Laihinen, E. Laakkonen, J. Lindén, J. Konu, H. Vrielinck, D. Van Der Heggen, P. F. Smet, T. L. Bahers, M. Lastusaari, *Chem. Mater.* **2020**, *32*, 8895.
[86] S. Vuori, P. Colinet, I. Norrbo, R. Steininger, T. Saarinen, H. Palonen, P. Paturi, L. C. V. Rodrigues, J. Göttlicher, T. Le Bahers, M. Lastusaari, *Adv. Opt. Mater.* **2021**, *9*, DOI https://doi.org/10.1002/adom.202100762.
[87] H. C. Byron, C. Swain, P. Paturi, P. Colinet, R. Rullan, V. Halava, T. Le Bahers, M. Lastusaari, *Adv. Funct. Mater.* **2023**, 2303398.
[88] D. Kodžoman, A. Hladnik, A. Pavko Čuden, V. Čok, *Color Res. Appl.* **2022**, *47*, 182.
[89] K. Niinimäki, G. Peters, H. Dahlbo, P. Perry, T. Rissanen, A. Gwilt, *Nat. Rev. Earth Environ.* **2020**, *1*, 189.
[90] B. K. Armstrong, A. Kricker, *Melanoma Res.* **1993**, *3*, 395.
[91] M. Saraiya, K. Glanz, P. A. Briss, P. Nichols, C. White, D. Das, S. J. Smith, B. Tannor, A. B. Hutchinson, K. M. Wilson, N. Gandhi, N. C. Lee, B. Rimer, R. C. Coates, J. F. Kerner, R. A. Hiatt, P. Buffler, P. Rochester, *Am. J. Prev. Med.* **2004**, *27*, 422.
[92] R. and N. S. A. STUK, "Ultraviolet radiation causes skin cancer," **2025**.

[93] K. Merin, M. Shaji, R. Kameswaran, *Indian J. Dermatol.* **2022**, *67*, 625.
[94] A. H. Fischer, T. S. Wang, G. Yenokyan, S. Kang, A. L. Chien, *J. Am. Acad. Dermatol.* **2016**, *75*, 371.
[95] M. B. Veierod, E. Weiderpass, M. Thorn, J. Hansson, E. Lund, B. Armstrong, H.-O. Adami, *JNCI J. Natl. Cancer Inst.* **2003**, *95*, 1530.
[96] B. Bao, J. Fan, Z. Wang, Y. Wang, W. Wang, X. Qin, D. Yu, *Compos. Part B Eng.* **2020**, *202*, 108464.
[97] E. Rehfuess, *Global Solar UV Index: A Practical Guide*, World Health Organization, Geneva, Switzerland, **2002**.
[98] V. Fioletov, J. B. Kerr, A. Fergusson, *Can. J. Public Health.* **2010**, *101*, I5.
[99] D. Selishchev, G. Stepanov, M. Sergeeva, M. Solovyeva, E. Zhuravlev, A. Komissarov, V. Richter, D. Kozlov, *Catalysts* **2022**, *12*, 1298.
[100] J. Liu, Y. Wang, J. Ma, Y. Peng, A. Wang, *J. Alloys Compd.* **2019**, *783*, 898.
[101] A. Nautiyal, S. R. Shukla, V. Prasad, *Cellulose* **2022**, *29*, 5923.
[102] H. Zhao, S. Wang, M. Zhou, Z. Cai, Y. Zhao, *J. Mater. Sci. Mater. Electron.* **2022**, *33*, 24706.
[103] X. Yang, D. Wang, *ACS Appl. Energy Mater.* **2018**, *1*, 6657.
[104] H. Tong, S. Ouyang, Y. Bi, N. Umezawa, M. Oshikiri, J. Ye, *Adv. Mater.* **2012**, *24*, 229.
[105] L. Cheng, Q. Xiang, Y. Liao, H. Zhang, *Energy Environ. Sci.* **2018**, *11*, 1362.
[106] N. Serpone, A. V. Emeline, *J. Phys. Chem. Lett.* **2012**, *3*, 673.
[107] M. A. Johar, R. A. Afzal, A. A. Alazba, U. Manzoor, *Adv. Mater. Sci. Eng.* **2015**, *2015*, 1.
[108] R. Rusdi, A. A. Rahman, N. S. Mohamed, N. Kamarudin, N. Kamarulzaman, *Powder Technol.* **2011**, *210*, 18.
[109] A. Khlyustova, N. Sirotkin, T. Kusova, A. Kraev, V. Titov, A. Agafonov, *Mater. Adv.* **2020**, *1*, 1193.
[110] W. Li, H. Zhang, W. Chen, L. Yang, H. Wu, N. Mao, *Cellulose* **2022**, *29*, 193.
[111] E. Hosono, S. Fujihara, T. Kimura, H. Imai, *J. Sol-Gel Sci. Technol.* **2004**, *29*, 71.
[112] K. Dai, S. Cao, J. Yuan, Z. Wang, H. Li, C. Yuan, X. Yan, R. Xing, *ACS Appl. Mater. Interfaces* **2025**, *17*, 30402.
[113] H. Jiang, L. Li, Z. Li, X. Chu, *Biomed. Microdevices* **2024**, *26*, DOI 10.1007/s10544-023-00686-8.
[114] G. Li, Y. Wang, L. Mao, *RSC Adv* **2014**, *4*, 53649.
[115] V. Batra, I. Kaur, D. Pathania, Sonu, V. Chaudhary, *Appl. Surf. Sci. Adv.* **2022**, *11*, 100314.
[116] J. Wojnarowicz, T. Chudoba, W. Lojkowski, *Nanomaterials* **2020**, *10*, 1086.
[117] A. Kołodziejczak-Radzimska, T. Jesionowski, *Materials* **2014**, *7*, 2833.
[118] Y. Sun, L. Chen, Y. Bao, Y. Zhang, J. Wang, M. Fu, J. Wu, D. Ye, *Catalysts* **2016**, *6*, 188.
[119] B. Lallo Da Silva, B. L. Caetano, B. G. Chiari-Andréo, R. C. L. R. Pietro, L. A. Chiavacci, *Colloids Surf. B Biointerfaces* **2019**, *177*, 440.
[120] K. T. Kim, M. Y. Eo, T. T. H. Nguyen, S. M. Kim, *Int. J. Implant Dent.* **2019**, *5*, 10.
[121] Y. He, M. Wan, Z. Wang, X. Zhang, Y. Zhao, L. Sun, *Surf. Coat. Technol.* **2019**, *378*, 125079.
[122] T. V. Arsha Kusumam, T. Panakkal, T. Divya, M. P. Nikhila, M. Anju, K. Anas, N. K. Renuka, *Ceram. Int.* **2016**, *42*, 3769.
[123] S. S. Alias, A. A. Mohamad, *Synthesis of Zinc Oxide by Sol–Gel Method for Photoelectrochemical Cells*, Springer Singapore, Singapore, **2014**.
[124] N. Talebian, S. M. Amininezhad, M. Doudi, *J. Photochem. Photobiol. B* **2013**, *120*, 66.
[125] L. Li, H. Yang, H. Zhao, J. Yu, J. Ma, L. An, X. Wang, *Appl. Phys. A* **2010**, *98*, 635.
[126] X. Jiaqiang, C. Yuping, C. Daoyong, S. Jianian, *Sens. Actuators B Chem.* **2006**, *113*, 526.
[127] C. Jiang, W. Liu, M. Yang, C. Liu, S. He, Y. Xie, Z. Wang, *Colloids Surf. Physicochem. Eng. Asp.* **2018**, *559*, 235.
[128] C. M. Chang, M. H. Hon, I. C. Leu, *Sens. Actuators B Chem.* **2010**, *151*, 15.
[129] N. Kaneva, I. Stambolova, V. Blaskov, Y. Dimitriev, A. Bojinova, C. Dushkin, *Surf. Coat. Technol.* **2012**, *207*, 5.

[130] S. V. Bhosale, M. Al Kobaisi, R. W. Jadhav, L. A. Jones, *Chem. Rec.* **2021**, *21*, 257.
[131] E. Mohammadi, M. Aliofkhazraei, M. Hasanpoor, M. Chipara, *Crit. Rev. Solid State Mater. Sci.* **2018**, *43*, 475.
[132] K. H. Guenther, *Thin Solid Films* **1981**, *77*, 239.
[133] B. Clarke, K. Ghandi, *Small* **2023**, 2302864.
[134] J. Wang, J. Zhao, L. Sun, X. Wang, *Text. Res. J.* **2015**, *85*, 1104.
[135] Y. Sun, W. Zhang, Q. Li, H. Liu, X. Wang, *Adv. Sens. Energy Mater.* **2023**, *2*, 100069.
[136] P. L. Mahapatra, P. Kumbhakar, B. Lahiri, S. K. Sinha, C. S. Tiwary, *Mater. Res. Bull.* **2022**, *146*, 111590.
[137] Z. Chen, J. Zhao, J. Chen, Y. Zhang, D. Chen, Q. Wang, D. Xia, *Sep. Purif. Technol.* **2021**, *258*, 118007.
[138] F. Yamin, F. Naddafiun, S. Zohoori, *J. Nat. Fibers* **2022**, *19*, 6770.
[139] C. Zhu, A. Mochizuki, J. Shi, M. Ishimori, S. Koyama, H. Ishizawa, J. Yan, H. Morikawa, *Cellulose* **2021**, *28*, 8139.
[140] A. Cerhan Haink, G. B. Basim, *KONA Powder Part. J.* **2021**, *38*, 269.
[141] A. Zare, *Res. J. Text. Appar.* **2022**, *26*, 238.
[142] L. Andreu, I. Sánchez, C. Mele, *J. Retail. Consum. Serv.* **2010**, *17*, 241.
[143] J. Wang, J. Shen, D. Ye, X. Yan, Y. Zhang, W. Yang, X. Li, J. Wang, L. Zhang, L. Pan, *Environ. Pollut.* **2020**, *262*, 114665.
[144] In *COVID-19 Sustain. Dev. Goals*, Elsevier, **2022**, pp. 31–52.
[145] In *Adv. Sustain. Mater.*, Elsevier, **2025**, pp. 455–469.
[146] N. Nasirzadeh, M. Monazam Esmaeelpour, N. Naseri, S. Omari Shekaftik, *Int. J. Environ. Health Res.* **2024**, *34*, 2067.
[147] *Sun Protective Clothing: Evaluation and Classification*, Standards Australia ; Standards New Zealand, Homebush, NSW, Wellington, N.Z., **1996**.
[148] T. Gambichler, J. Laperre, K. Hoffmann, *J. Eur. Acad. Dermatol. Venereol.* **2006**, *20*, 125.
[149] L. Doveri, Y. A. Diaz Fernandez, G. Dacarro, *ACS Omega* **2024**, *9*, 25575.
[150] B. Xu, M. Ganesan, R. K. Devi, X. Ruan, W. Chen, C. C. Lin, H. Chang, E. Lizundia, A. K. An, S. K. Ravi, *Adv. Mater.* **2025**, *37*, 2406666.
[151] A. Yao, X. Jiao, D. Chen, C. Li, *ACS Appl. Mater. Interfaces* **2020**, *12*, 18437.
[152] W. Liu, W. Cheng, M. Zhou, B. Xu, P. Wang, Q. Wang, Y. Yu, *Cellulose* **2022**, *29*, 7477.
[153] W. Liu, Y. Yu, W. Cheng, M. Zhou, L. Cui, P. Wang, Q. Wang, *Colloids Surf. B Biointerfaces* **2022**, *219*, 112829.
[154] X. Li, H. Wang, S. Yuan, S. Lin, S. Deng, Z. Du, X. Cheng, X. Du, *Polymer* **2022**, *250*, 124885.
[155] Y. Fang, G. Chen, M. Bick, J. Chen, *Chem. Soc. Rev.* **2021**, *50*, 9357.
[156] F. Cai, T. Song, B. Yang, X. Lv, L. Zhang, H. Yu, *Chem. Mater.* **2021**, *33*, 9750.
[157] H. Liu, H. Shen, H. Zhang, X. Wang, *J. Energy Storage* **2022**, *49*, 104158.
[158] S. Hao, W. Zhang, J. Weng, J. Yao, J. Li, X. Li, *J. Ind. Text.* **2022**, *51*, 6797S.
[159] H. Wang, Y. Feng, J. Gao, W. Fang, J. Ge, X. Yang, F. Zhai, Y. Yu, W. Feng, *Adv. Sci.* **2022**, *9*, 2201657.
[160] Q. Ren, N. Yu, P. Zou, Q. He, D. K. Macharia, Y. Sheng, B. Zhu, Y. Lin, G. Wu, Z. Chen, *Chem. Eng. J.* **2022**, *441*, 136043.
[161] S. Mitsuzawa, S. Deguchi, K. Horikoshi, *FEMS Microbiol. Lett.* **2006**, *260*, 100.
[162] A. Menichetti, D. Mordini, M. Montalti, *Int. J. Mol. Sci.* **2024**, *25*, 8975.
[163] P. Kumar, S. Roy, A. Sarkar, A. Jaiswal, *ACS Appl. Mater. Interfaces* **2021**, *13*, 12912.
[164] G. Stoychev, A. Kirillova, L. Ionov, *Adv. Opt. Mater.* **2019**, *7*, DOI 10.1002/adom.201900067.
[165] S. Huang, Y. Shen, H. K. Bisoyi, Y. Tao, Z. Liu, M. Wang, H. Yang, Q. Li, *J. Am. Chem. Soc.* **2021**, *143*, 12543.
[166] J. Chen, S. Sun, M. M. Macios, E. Oguntade, A. R. Narkar, P. T. Mather, J. H. Henderson, *ACS Appl. Mater. Interfaces* **2023**, *15*, 50962.
[167] L. Yang, Z. Wang, G. Fei, H. Xia, *Macromol. Rapid Commun.* **2017**, *38*, 1700421.

[168] O. Kuksenok, A. C. Balazs, *Mater. Horiz.* **2016**, *3*, 53.
[169] Y. Zhang, X. Wang, X. Zhang, W. Wang, Y. Yao, J. Pan, G. Shao, S. Bi, N. Chen, J. Jiang, H. Shao, *Mater. Horiz.* **2025**, *12*, 4862.
[170] J. Xiong, J. Chen, P. S. Lee, *Adv. Mater.* **2021**, *33*, DOI 10.1002/adma.202002640.
[171] N. Yan, Z. Zheng, Y. Liu, X. Jiang, J. Wu, M. Feng, L. Xu, Q. Guan, H. Li, *Nano Res.* **2022**, *15*, 1383.
[172] F. Ahangaran, A. H. Navarchian, F. Picchioni, *J. Appl. Polym. Sci.* **2019**, *136*, 48039.
[173] T. Yimyai, A. Pena-Francesch, D. Crespy, *Macromol. Rapid Commun.* **2022**, *43*, DOI 10.1002/marc.202200554.
[174] W. Du, Y. Jin, S. Lai, L. Shi, W. Fan, J. Pan, *Polymer* **2018**, *158*, 120.
[175] J. T. Kim, B. K. Kim, E. Y. Kim, S. H. Kwon, H. M. Jeong, *Eur. Polym. J.* **2013**, *49*, 3889.
[176] C. Li, P. Wang, D. Zhang, S. Wang, *ACS Appl. Mater. Interfaces* **2022**, *14*, 45988.
[177] P. Meganathan, S. Subbaiah, L. M. Selvaraj, V. Subramanian, S. Pitchaimuthu, N. Srinivasan, *Phosphorus Sulfur Silicon Relat. Elem.* **2022**, *197*, 244.
[178] N. Sarwar, U. Bin Humayoun, M. Kumar, A. Nawaz, M. S. Zafar, U. Rasool, Y. H. Kim, D. H. Yoon, *Mater. Lett.* **2022**, *309*, 131338.
[179] M. A. Alvarez-Amparán, V. Martínez-Cornejo, L. Cedeño-Caero, K. A. Hernandez-Hernandez, R. D. Cadena-Nava, G. Alonso-Núñez, S. F. Moyado, *Appl. Nanosci.* **2022**, *12*, 4019.
[180] B. Yan, Y. Ren, S. Ding, M. Zhou, L. Cui, Y. Yu, Q. Wang, B. Xu, P. Wang, *Compos. Commun.* **2022**, *34*, 101260.
[181] H. K. Woo, K. Zhou, S. Kim, A. Manjarrez, M. J. Hoque, T. Seong, L. Cai, *Adv. Funct. Mater.* **2022**, *32*, 2201432.
[182] Y. Wang, D. Shou, S. Shang, K.-L. Chiu, S. Jiang, *Sol. Energy* **2022**, *233*, 196.
[183] M. Shi, M. Shen, X. Guo, X. Jin, Y. Cao, Y. Yang, W. Wang, J. Wang, *ACS Nano* **2021**, *15*, 11396.
[184] S. Vuori, Reversible Photochromism of Synthetic Hackmanites in Radiation Detection and Quantification, University of Turku, **2023**.
[185] S. Vuori, P. Colinet, J.-P. Lehtiö, A. Lemiere, I. Norrbo, M. Granström, J. Konu, G. Ågren, P. Laukkanen, L. Petit, A. J. Airaksinen, L. Van Goethem, T. Le Bahers, M. Lastusaari, *Mater. Horiz.* **2022**, *9*, 2773.
[186] N. Aldegunde-Louzao, M. Lolo-Aira, C. Herrero-Latorre, *Environ. Toxicol. Pharmacol.* **2024**, *108*, 104457.
[187] A. Zorzoli, A. MacLean, S. Nicholson, A. Daniels, S. Hughes, S. Bennet-Slater, C. Tait-Burkard, N. E. Sakka, R. Gunson, K. Templeton, *BioTechniques* **2024**, *76*, 295.
[188] S. Moungsrijun, S. Sujinnapram, S. Sutthana, *Monatshefte Für Chem. - Chem. Mon.* **2017**, *148*, 1177.
[189] R. Herrera-Rivera, M. de la L. Olvera, A. Maldonado, *J. Nanomater.* **2017**, *2017*, 1.
[190] S. Vuori, T. Laine, I. Norrbo, J. Holvitie, M. Lastusaari, **2024**.
[191] C. R. Osterwald, T. J. McMahon, *Prog. Photovolt. Res. Appl.* **2009**, *17*, 11.
[192] R. Paul, *High Performance Technical Textiles*, Wiley, **2019**.
[193] N. Kanari, D. Mishra, I. Gaballah, B. Dupré, *Thermochim. Acta* **2004**, *410*, 93.
[194] S. Afzal, W. A. Daoud, S. J. Langford, *Appl. Surf. Sci.* **2013**, *275*, 36.
[195] S. Ghayempour, M. Montazer, *Ultrason. Sonochem.* **2017**, *34*, 458.
[196] M. A. Tănase, A. C. Soare, P. Oancea, A. Răducan, C. I. Mihăescu, E. Alexandrescu, C. Petcu, L. M. Diţu, M. Ferbinteanu, B. Cojocaru, L. O. Cinteza, *Nanomaterials* **2021**, *11*, 2574.
[197] A. Šarić, I. Despotović, G. Štefanić, *J. Phys. Chem. C* **2019**, *123*, 29394.
[198] A. Umar, R. Kumar, G. Kumar, H. Algarni, S. H. Kim, *J. Alloys Compd.* **2015**, *648*, 46.
[199] S. Shrestha, B. Wang, P. Dutta, *Adv. Colloid Interface Sci.* **2020**, *279*, 102162.
[200] Z. Qi, K. Wang, J. Chen, D. Gao, Y. Ren, C. Wang, *New J. Chem.* **2021**, *45*, 11119.
[201] O. K. Alebeid, T. Zhao, *J. Text. Inst.* **2017**, *108*, 2027.

[202] N. S. Heliopoulos, G. N. Kouzilos, A. I. Giarmenitis, S. K. Papageorgiou, K. Stamatakis, F. K. Katsaros, *Fibers Polym.* **2020**, *21*, 1238.
[203] M. T. Noman, J. Militky, J. Wiener, J. Saskova, M. A. Ashraf, H. Jamshaid, M. Azeem, *Ultrasonics* **2018**, *83*, 203.
[204] M. Yatagai, S. H. Zeronian, *Cellulose* **1994**, *1*, 205.
[205] S. Staniforth, T. T. Schaeffer, *Stud. Conserv.* **2004**, *49*, 213.
[206] R. Nizamov, J. Kaschuk, Y. Al Haj, M. Nyberg, M. Imani, E. Pasquier, O. Rojas, T. Abitbol, J. Vapaavuori, K. Miettunen, *Cellulose* **2025**, DOI 10.1007/s10570-025-06380-7.
[207] J. Valdez Garcia, A. Boding, X. Yang, R. Nizamov, M. S. Reid, K. Junel, K. Miettunen, T. Abitbol, J. Kaschuk, *Int. J. Biol. Macromol.* **2025**, *292*, 139203.
[208] L. Karttunen, S. Jouttijärvi, A. Poskela, H. Palonen, H. Huerta, M. Todorović, S. Ranta, K. Miettunen, *Renew. Energy* **2023**, *219*, 119473.
[209] G. K. Grandhi, G. Koutsourakis, J. C. Blakesley, F. De Rossi, F. Brunetti, S. Öz, A. Sinicropi, M. L. Parisi, T. M. Brown, M. J. Carnie, R. L. Z. Hoye, P. Vivo, *Nat. Rev. Clean Technol.* **2025**, DOI 10.1038/s44359-024-00013-1.
[210] E. I. Bernhofer, P. A. Higgins, B. J. Daly, C. J. Burant, T. R. Hornick, *J. Adv. Nurs.* **2014**, *70*, 1164.
[211] D. S. R. Rahayu, M. R. Mak'ruf, S. Syaifudin, *Int. J. Adv. Health Sci. Technol.* **2021**, *1*, 20.
[212] J. Iwamoto, K. Obayashi, M. Kobayashi, T. Kotsuji, R. Matsui, K. Ito, O. Yoshida, N. Kurumatani, K. Saeki, *Chronobiol. Int.* **2018**, *35*, 719.
[213] L. Pompei, L. Blaso, S. Fumagalli, F. Bisegna, *Energy Build.* **2022**, *263*, 112025.
[214] U.S. Energy Information Administration, *How Much Electricity Is Used for Lighting in the United States?*, Eia.Gov, **2024**.
[215] G. Gereffi, *J. Int. Bus. Policy* **2020**, *3*, 287.
[216] L.-G. Ding, S. Wang, B.-J. Yao, W.-X. Wu, J.-L. Kan, Y. Liu, J. Wu, Y.-B. Dong, *J. Mater. Chem. A* **2022**, *10*, 3346.
[217] A. Schmitz, R. Stamminger, *Energy Effic.* **2014**, *7*, 937.
[218] I. G. Klepp, K. Laitala, S. Wiedemann, *Sustainability* **2020**, *12*, 6219.
[219] *A New Textiles Economy: Redesigning Fashion's Future*, Ellen MacArthur Foundation, **2017**.

TURUN
YLIOPISTO
UNIVERSITY
OF TURKU

Painosalama, Turku, Finland 2025

ISBN 978-952-02-0468-6 (PRINT)
ISBN 978-952-02-0469-3 (PDF)
ISSN 2736-9390 (Print)
ISSN 2736-9684 (Online)